Summer 2016

Artificial neural network approach to predict blast-induced ground vibration, airblast and rock fragmentation

Raymond Ninnang Tiile

Department:

ARTIFICIAL NEURAL NETWORK APPROACH TO PREDICT BLAST-INDUCED GROUND VIBRATION, AIRBLAST AND ROCK FRAGMENTATION

by

RAYMOND NINNANG TIILE

A THESIS

Presented to the Faculty of the Graduate School of the

MISSOURI UNIVERSITY OF SCIENCE AND TECHNOLOGY

In Partial Fulfillment of the Requirements for the Degree

MASTER OF SCIENCE IN MINING ENGINEERING

2016

Approved by

Dr. Nassib Aouad, Advisor

Dr. Maochen Ge

Dr. Greg Galecki

ABSTRACT

Blasting has been widely used as an economical and cheap way of rock breakage in mining and civil engineering applications. An optimal blast yields the best fragmentation in a safe, economic and environmentally friendly manner. The degree of fragmentation is vital as it determines to a large extent the utilization of equipment, productivity and mill throughput. Explosive energy, besides rock fragmentation, creates health and safety issues such as ground vibration, air blast, fly rock, and back breaks among others. As a result, the explosive energy impacts structures and buildings located in the vicinity of the blasting operation, and causes human annoyance, as well as exposes operators in the field to hazardous conditions. There is therefore a need to develop a model to predict blast-induced ground vibration (PPV), airblast (AOp), and rock fragmentation. Artificial neural network (ANN) technique is preferred over empirical and other statistical predictive methods as it is able to incorporate the numerous factors affecting the outcome of a blast. This study seeks to develop a simultaneous integrated prediction model for rock fragmentation, ground vibration and air blast using MATLAB-based artificial neural network system. Training, validation and testing was done with a total of 180 monitored blast records taken from a gold mining company in Ghana using a three-layer, feed-forward back-propagation ANN.

Based on the results obtained from the study, ANN model with architecture of 7-13-3 was found optimum having the least root mean square error (RMSE) of 0.307. Artificial neural network (ANN) technique has been compared to empirical and conventional statistical methods. Sensitivity analysis has also been conducted to ascertain the relative influence of each input parameter on rock fragmentation, PPV and AOp.

ACKNOWLEDGMENTS

I am highly indebted to my advisor, Dr. Nassib Aouad, for his technical knowledge, inspiration and support leading to the successful completion of my research. I am most grateful to you for funding my research program. I would like to thank the examining committee members: Dr. Maochen Ge, and Dr. Greg Galecki, both of the Mining Engineering department of Missouri S&T, for their support and guidance. I am also grateful to all the faculty members of Mining Engineering department of Missouri S&T for their advice and assistance during my research.

Further, I extend my appreciation to Perseus Mining Limited (Ghana) especially Mr. Jesse Bukroh and Mr. Abraham Benin for their technical assistance when hard decisions had to be made. To Mrs. Tina Alobaidan, Ms. Shirley Hall and Ms. Judy Russell I say thank you for the role you played during my study.

Special thanks to my friend Francis Arthur and to the entire Ghanaian family here in Rolla for their diverse support and prayers. To Victoria my lovely Wife I say well done for the encouragement, advice and love shown me throughout my graduate studies.

I am extremely thankful to my family, especially my father, Mr. George Tiile for their prayers and support during this period.

Lastly but not the least, gratitude goes to all who directly or indirectly helped me in one way or the other during the period.

TABLE OF CONTENTS

LIST OF FIGURES

Page

LIST OF TABLES

Page

1. INTRODUCTION

1.1. BACKGROUND

Rock fragmentation is a fundamental mining activity that affects the downstream processes; hence, there is a need of optimizing fragmentation. Optimizing rock fragmentation results in (i) maximizing crusher throughput; (ii) improving excavator productivity; (iii) minimizing equipment (i.e. excavator and crusher) maintenance and repair costs. After the rocks are fragmented, the excess explosive energy creates ill effects such as ground vibration, air blast, fly rock, and back breaks among others. Air blast and ground vibration are usually potential causes of property damage and human annoyance. Effective control of airblast and ground vibration avoids persistent complains from affected inhabitants and prevents property damages to surrounding area.

A number of conventional statistical, empirical equations and artificial neural network systems have been employed by various researchers to predict rock fragmentation, ground vibration and airblast prior to blasting operations. However, artificial neural network (ANN) is preferred over the other predictive techniques due to its ability to incorporate the numerous factors affecting the outcome of a blast among other advantages. However, the ANN model generated is site specific, the input parameters can be expanded to include mechanical and geotechnical rock parameters such as rock strength, RQD, rock hardness, number of joints etc. to provide the ANN model a wider application. Thus, for this research, the ANN system is used to generate an optimum model for predicting blast-induced ground vibration, airblast and rock fragmentation.

Artificial neural networks (ANN) are structures of interconnected neurons and usually involve the exchange of signals between neurons. ANN systems are good at non-linear fittings as well as recognizing patterns after a successful training process and outputs can be predicted given new sets of inputs.

1.2. STATEMENT OF THE PROBLEM

Blasting operations often focus on controlling fragmentation while neglecting the environmental consequences. An optimal blast yields the desired fragmentation in a safe, economic and environmentally friendly manner. On the other hand, a poorly conducted blast would typically result in poor fragmentation and ill effects such as fly rocks, ground vibration, airblast and back break. Among these nuisances, ground vibration and airblast are the potential causes of property damages and noise pollution as noted in a case study conducted at an open pit gold mine located in Ghana. The mining company had been in successful business until recently. Complaints from inhabitants over noise and cracks developed in their buildings comes in the wake of poor excavator productivities, reduced crusher throughput, low crusher and excavator availabilities, and overall reduction in ounces realized. Results of investigations conducted proved that the blasting operations caused the cracks in neighboring structures. Poor fragmentation caused relatively lower excavator productivities, wear and damages to crusher and excavator teeth, reduced crusher throughput, and overall reduction in ounces produced. There was therefore an urgent need for solutions to the blast-related problems.

An attempt was made to improve the blasts results using empirical models. These empirical models were generally unsuccessful due to their inability to address the internal complexities in the input parameters. Moreover, they allowed limited inputs and were unable to predict multiple outputs. To address the above-mentioned weaknesses of the empirical predictors and to resolve the blast-related challenges, artificial neural network (ANN) was used. Classical examples of poor fragmentation at the mine are presented in Figures 1.1 and 1.2 below.

Figure 1.1. Rock formation stationary after blasting

Figure 1.2. Visible rock formation after blasting

1.3. PROJECT OBJECTIVES

Optimized blasts generate the desired fragmentation and minimize the impact of ground vibration and airbast on the neighborhood of the blasting operations. This research focuses on four main objectives in order to improve rock fragmentation. These objectives are to:

- Develop an integrated prediction model for rock fragmentation, blast-induced ground vibration and airblast using MATLAB-based artificial neural network system.
- Compare artificial neural network (ANN) predictions to conventional statistical (multivariate regression analysis) and other empirical methods to define the best approach.
- Carry out sensitivity analysis on all input parameters to ascertain the relative influence of each parameter on rock fragmentation, ground vibration (PPV) and airblast (AOp).
- Use optimum ANN model generated to achieve desired fragmentation under environmentally acceptable limits.

1.4. MINE BACKGROUND INFORMATION

1.4.1. Location and Accessibility. The Mine is located in Ghana, West Africa. It is approximately 57 km to the south-west of Obuasi and 195 km north-west of the capital Accra on the eastern flank of the prospective Ashanti Belt and 16 km west of Dunkwa, near Ayanfuri. The Mine lies between latitude 1°50’00” and 2°00’00’’ and longitude 5°48’49’’ and 6°00’00”. It can be accessed by a 107 km road from Kumasi, which lies to the north of the mine and a 186 km road from the port of Takoradi south of the mine. The Dunkwa/Awaso defunct railway line passes 2 km north east of the mine.

1.4.2. Mine Geology. The deposits occur near the western flank of the Ashanti Greenstone Belt. Numerous small Basin-type or Cape Coast-type granite bodies have intruded the sediments along several regional structures. The intrusive shapes vary from nearly ovoid plugs 200 m to 400 m long by 40 m to 150 m wide to relatively long (+2,000 m) narrow (50 m -100 m) sills or dykes. Gold mineralization has been identified in a single granitoid intrusive over an open strike of 2 km between Abnabna and Fobinso

pits. Most of the gold mineralization is contained within five (5) zones. These main zones range from 30 m to 140 m in width and have a moderate to steep northerly plunge.

1.4.3. Mine Operations. The gold mine practices open pit mining method to extract ore in two main productive pits. Mining is selective with bulk waste stripping on 5m and 10m benches. Mining operation runs a two-shift system with 10 hours per shift. Full capacity commercial production started in 2011 and the mine still has over 10 years mine life. The mining operation begins with drilling of holes, loading the holes with explosives and blasting. After the rocks are fragmented, they are loaded into haul trucks using excavators. Ore is hauled to the stockpile or direct-tipped into crusher while the waste rock taken to the waste dump. As mining progresses, it is necessary to dewater the mine to ensure that the water level remains below the pit floor. Thousands of gallons of water are pumped from the pit each day. Much of the water is reused on site to control dust. Surplus water is treated and discharged back into nearby rivers.

1.4.4. Drilling and Blasting. Sandvik DP1500 hydraulic rigs are used for drilling. Blast holes with diameters of 115 mm are drilled vertically to depths of 5m, 7.5m and 10m. A 3.2 m x 3.7 m and a 3.5 m x 4.1 m staggered drill pattern are used for the ore and waste shots respectively.

Ammonium nitrate fuel oil, ANFO (P100 bulk emulsion) with average density of 1.13 g/cm^3 is used as the main blasting agent and the detonating cord as initiation system. Priming is carried out using non-electric (NONEL) detonators and pentolite cartridges. The inter hole delays are 17ms or 25ms and the inter row delays are 42ms or 67ms.

1.4.5. Material Handling. Loading is done mainly by two Liebherr 9250 and two Liebherr 984 excavators in 5 m lifts and 10 m lifts depending on the type of material being loaded. Two Liebherr 984 excavators are used to supplement production in times of unscheduled breakdowns. Each excavator is assigned five or six Caterpillar 777D dump trucks in a single back-up spotting configuration depending on the haul road distance. The haul roads have average grades of 0 to 10% that lead to three main active dumps. These main dumps are the oxide and transition waste dump, the Run-of-Mine (ROM) pad or the crusher and the tailings embankment dump. Figure 1.3 illustrates one of the operational pits in the mine.

Figure 1.3. Active pit view

1.4.6. Ore Processing. A 5.5 Mtpa carbon-in-leach (CIL) plant composed of primary gyratory crushers is used in the mineral processing. Once the ore is mined, it is fed to crushers and grinding mills to reduce the size of the ore and expose the gold. Water is added in the process to form slurry. This slurry is then passed on to leaching tanks where cyanide solution is added to leach the gold into the solution. Carbon granules are put into solution for gold attachment. The gold is then stripped from the carbon granules and the gold bearing solution pumped through electro-winning cells to extract the gold. The gold undergoes smelting in a furnace to form the liquid gold that later hardens to form bullion bars. These bullion gold bars contain about 60 to 95% gold for this reason the gold bars are send to a refinery for further processing into pure gold.

1.5. SUMMARY

This research work produces an optimum artificial neural network (ANN) model that has the ability to optimize blasting operations. Optimized blasts yield desired fragmentation leading to maximized crusher throughput, improved excavator productivity, and reduced equipment maintenance and repair costs. Optimizing blasting operations also prevent or minimize the impact of ground vibration and airbast on the neighborhood of the blasting operations preventing property damage and human annoyance. Section 2 reviews literature on blasting and ANN.

2. LITERATURE REVIEW

2.1. BLASTING

Blasting in an open pit mine starts by generating a blast design. A number of factors should be considered when designing a blast and include fragmentation needs, geology, nearby structures, integrity of walls, explosive type, vibration and airblast considerations, and type of drilling equipment. Consideration should also be given to adequate confinement and availability of enough room for rocks to break into. Blast design parameters are estimated based on empirical formulas and experience. The Blast parameters are burden, spacing, hole depth, hole diameter, sub-drill, stemming height, charge length, and powder factor among others. After designing the blast, it is set out on the ground for drilling. Figure 2.1 is an example of a blast design

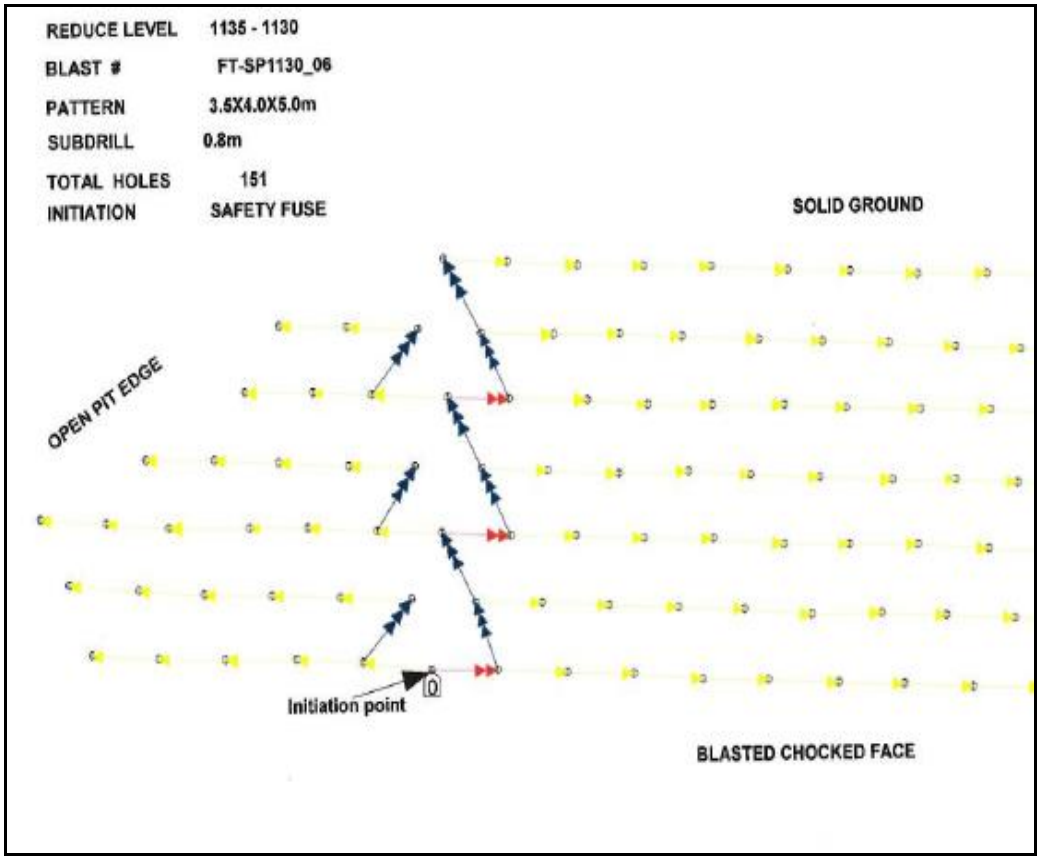

Figure 2.1. Blast design

Drilling pattern is set out on the field and drilling of holes started. The blast holes are drilled to required depths and loaded with appropriate explosives. The surface connections done using the right delays and blasting initiated. Best blasting results are achieved by paying close attention to the drilling and blasting process.

When a charge explodes, it generates high-pressure, high-temperature gases against the containing borehole thus creating a strain field in the rock. The drill hole pressure build-up depends on the physical characteristics of the rock and explosive composition. The shockwave initiates the fragmentation process once it contacts the drill hole wall. The immediate surrounding rock is crushed when the compressive strength of the rock is exceeded. Beyond the crushed zone, surrounding rocks develop radial cracks as the shockwave intensity exceeds the tensile strength of rock. The resulting gas pressure travels through the cracks extending them further. The shockwaves radiating from the drill hole are converted to tensile waves when they encounter a free face.

Blasting has been the cheapest means of rock breakage in the mining industry. It is a vital step to the entire mining operation. Competence of all the subsystems (e.g. loading, hauling and crushing) is dependent on the fragmentation quality (Mackenzie 1966; Monjezi et al., 2010). Optimum size distribution can enhance the overall mine/plant economics (Hustrulid, 1999; Michaux and Djordjevic, 2005; Kanchibotla, 2001; Morin and Francesco 2006; Monjezi et al., 2010). Every blast regardless of the design would produce a certain amount of unwanted energy that radiates from the blast area in the form of ground vibrations and airblast (Hagan, 1973). Airblast and ground vibrations cause objects to rattle making noise, as well as results in vibration of structures in the neighboring premises. Excessive ground vibration can also affect the groundwater, and ecology of the nearby area (Khandelwal and Singh, 2009). Proper control of blasting practices is therefore necessary to ensure both the safety of employees and the protection of the community from adverse effects. To prevent and reduce the adverse effect of blasting operation, special attention should be given to the generation and propagation mechanism of blast-induced ground vibrations (McKenzie, 1990).

Ground vibration usually reaches structure foundations before airblast pressure does because of different wave propagation velocities in geomaterials and in the air. Airblast and ground vibrations might act on the structure simultaneously, depending on

the distance between the explosion center and the structure. Hence, proper analysis of structure response and damage to a nearby surface explosion should take into accounts both ground shock and airblast pressure (Wu and Hao, 2007).

A number of damage criteria have been established to enhance blasting efficiency (Duvall et al., 1963; Nicholls eta al., 1971; Siskind et al., 1989; Elseman and Rasoul, 2000). Adequate airblast and ground vibration standards have been set by many countries to avoid structural damages and to reduce human complaints. Thus, blasting activities are to be planned and conducted to comply with these standards.

2.2. BLAST-INDUCED GROUND VIBRATION

An important environmental aspect of mining is the evaluation of blast- induced ground vibration transmitted through the ground. Railways, highway traffic and machinery in nearby locations are other potential sources of ground vibration. When transmitted ground vibrations strike the face of buildings, they impart momentum to the exterior components of the building. The kinetic energy of these transmissions are converted to strain energy in the structure causing partial damage to the extent of complete collapse of structure (Dusenberry, 2010). These Ground vibrations take the form of propagating waves that travel in the rock or soil away from the blast zone. Ground vibrations are associated with mostly Rayleigh waves, longitudinal waves and shear waves propagating through the ground. These wavelengths are influenced by both controllable and uncontrollable factors. The controllable factors include the pattern, hole depth, stemming length, and the charge column among others. On the other hand, the uncontrollable factors are rock conditions, geology and rock properties (Mohamed, 2009). Ground vibration is directly related to the quantity of explosive used and the distance between blast face to the monitoring point (Khandelwal and Singh, 2009).

A small amount of energy is converted into ground vibration in a properly designed blast, with great deal of energy used in fragmenting and throws of rock. Immediately surrounding the detonating hole is a crater zone, where the rock has been fractured and displaced by the shockwave and by the pressure of the hot gasses produced during the combustion process. Outside this crater zone, the shockwave is propagated through the medium as elastic waves. The energy transmitted from particle to particle

within rocks is termed as ground vibration. These waves radiating outward are categorized as body waves traveling through the ground and surface waves traveling on the surface of the ground. These body waves travel outwards in a spherical manner until they reach a boundary between two materials. At the intersection point, shear and surface waves are generated. A common type of the surface wave is the Rayleigh wave and is associated with energy flow along the surface. This wave arrives after the compression and shear wave as it has a relatively lower phase velocity. The Rayleigh wave is very important as it suffers less geometric spreading loss than body waves. In general, the amplitude of the vibration decreases with increasing distance away from the center of action due to diminishing energy levels.

Parameters often used to define the magnitude of ground vibration at any location are as follows:

- Particle displacement: The distance a particle moves before returning to its original position (measured in mm).
- Particle velocity: This is the rate of change of displacement (measured in mm/s).
- Particle acceleration: This is the rate of change of velocity (measured in mm/s^2).
- Frequency: This is the number of oscillations per second that a particle undergoes (measured in Hz).

Peak particle velocity (PPV) has been used in practice for the measurement of blast damage to structures. Some of the proposed damage criteria that are established mainly on the peak particle velocity (PPV mm/s) are presented in Table 2.1 (Nateghi, 2012). These recommendations are based on author experiences for blast-induced vibration limits near different types of structures in urban areas and are different for the same structures found in different countries (Pal, 2005).

Table 2.1. Suggested damage criteria

Predictor	Effects and damage	Maximum allowable PPV (mm/s)
Longefors et al. (1958)	No damage	<50
	Fine crack	100
	Cracks	150
	Serious cracks	225
Edwards and Northwood (1960)	Safe zone	<50
	Damage zone	100–150
Duvall and Fogleson (1962)	Major damage (95%)	50
Nicholls and Johnson (1971)	Safe zone (%95)	>50
	Damage zone	<50
Indian standard (1973)	Soil, weathered or soft rock	70
	Hard rock conditions	100

Predicting the transmission of blast-induced vibration through the ground is complex due to lack of complete understanding of rock behavior and the difficulty of determining accurate values of rock properties. In spite of these and other difficulties, reasonable assessments of blast-induced ground vibration can be achieved with the empirical, statistical and artificial intelligent techniques. Several empirical models have been developed by various researchers (Duvall and Fogleson, 1962; Duvall et al., 1963; Langefors and Kihlstrom, 1963; Birch and Chaffer, 1983; Davies et al., 1964; Ghosh and Daemen, 1983; Ambraseys and Hendron, 1968; and Bureau of Indian Standard, 1973) for predicting particle peak velocity. For most of these empirical predictors, the peak particle velocity (PPV) is the parameter of concern.

Peak particle velocity (PPV) is a function of the borehole pressure, confinement, charge weight, distance from blast area, manner of decay of compressive waves through rockmass and the effect of firing sequence of adjacent holes. All the predictors estimate the PPV mainly based on the maximum charge per delay and the distance between blast face and monitoring point. There is no uniformity in the predicted result since different

predictors give different values of PPV for various amount of allowable charge per delays in the same operating area. These predictors are not able to predict other important parameters such as frequency, air over pressure, and fly rocks (Dowding, 1985; Khandelwal and Singh, 2007; and Monjezi et al., 2011). Moreover, empirical methods are unable to incorporate the numerous factors that affect the PPV and their complex interrelationships, paving way for other techniques. Hence, approaches such as artificial neural network (ANN), Support Vector machines (SVM), Genetic Algorithm (GA) and Maximum likelihood classification are recently in use (Khandelwal, 2010). Table 2.2 presents some empirical predictor models.

Table 2.2. Empirical predictor equations

Names	**Equation**
USBM (1959)	$V=K[R/Qmax]^{-B}$
Langefors–Kihlstrom (1963)	$V=K[(Qmax/R^{2/3})^{1/2}]^{B}$
Ambraseys–Hendron (1968)	$v = K[R/(Qmax)^{1/3}]^{-B}$
Bureau of Indian Standard (1973)	$v = K[(Qmax/R^{2/3})]^{B}$

Recently, artificial neural network (ANN) has been employed extensively to predict blast induced ground vibration. Yong (2005) gave a comprehensive research program on the effect of various input variables on ground shock. The ANN technique was then applied to identify the system pattern and serve as a function for predicting the blast-produced ground vibration. The neural network approach could predict the unseen test data consistently with reasonable accuracy, thus deemed successful. He also

demonstrated that the directional angle, in addition to the scaled distance, is a crucial factor influencing the ground shock at a particular target point.

Khandelwal and Singh (2006) devised a neural network approach for predicting ground vibration and frequency by all impelling parameters of rock mass, explosive characteristics and blast design. This network was trained by 150 dataset with 458 epochs and 20 datasets tested. The suitability of this method was examined by comparing artificial neural network (ANN) with a conventional statistical relation. The correlation coefficient determined by ANN for peak particle velocity (PPV) and frequency were relatively higher than the correlation coefficient determined by statistical analysis.

Khandelwal and Singh (2007) considered the prediction of blast-induced ground vibration level at a Magnesite Mine in tecto-dynamically vulnerable hilly terrain in Himalayan region in India. The ground vibrations were observed to calculate the safe charge of explosive to avoid continuous complaints from nearby villagers. A total of 150 blast data sets was considered. Based on this study, it was established that the feed-forward back-propagation neural network approach seems to be the better option for predicting PPV to protect surrounding environment and structures.

Khandelwal and Singh (2009) investigated and predicted blast-induced ground vibration and frequency in a coal mine in india based on some parameters using ANN technique. A three-layer, feed-forward back-propagation neural network having 15 hidden neurons, 10 input parameters and two output parameters were trained using 154 experimental and monitored blast records. Results were then compared using correlation and mean absolute error (MAE) for monitored and predicted values of PPV and frequency. They concluded that ANN results for the PPV and frequency were very close to the field data sets compared to the conventional predictors and MVRA predictions.

Monjezi et al. (2010) presented the prediction of blast-induced ground vibration using various types of neural networks such as multi-layer perceptron neural network (MLPNN), radial basis function neural network (RBFNN) and general regression neural network (GRNN) in Sarcheshmeh copper mine, Iran. MLPNN gave the best results with root mean square error and coefficient of correlation of 0.03 and 0.954 respectively. Furthermore, Sensitivity analysis disclosed that distance from the blast, number of holes

per delay and maximum charge per delay are the most effective parameters in blast induced ground vibration analysis.

Artificial neural networks (ANN), Multi-variate regression analysis (MVRA) and empirical, analysis have been used by Kamali and Ataei (2010) to predict the blast-induced PPV in the structures of the Karoun III power plant and dam. The best model was the ANN since its outputs were highly correlated to the measured and observed data.

Monjezi et al. (2011) developed a predictive model for blast-induced ground vibration using artificial neural network (ANN) in the Siahbisheh project, Iran. Input parameters like maximum charge per delay, distance from blasting face to the monitoring point, stemming and hole depth were considered. From the prepared database, 162 datasets were used for the training and testing of the network, 20 randomly selected datasets were used to validate the ANN model. A four-layer feed-forward back-propagation neural network with architecture 4-10-5-1 was found to be optimum. The ANN model was compared with empirical predictors as well as regression analysis for performance. The comparison results showed that the ANN model demonstrated a high level of performance over the empirical predictors and statistical model. It was also realized from sensitivity analysis that the distance from blasting face to the monitoring point was the most effective parameter on PPV and stemming the least effective parameter on the PPV.

Application of soft computing to predict blast-induced ground vibration was the focus of research by Khandelwal et al. (2011). A Total of 130 experimental and monitored blast records from surface coal mines at different locations were trained and tested on a three-layer feed-forward back-propagation neural network with 2-5-1 architecture. Results were compared based on coefficient of determination and mean absolute error between monitored and predicted values of PPV. Based on this study, it was established that the feed-forward back-propagation neural network approach was the best option for close and appropriate prediction of PPV.

Gao et al. (2012) implemented ANN to develop a predictive model for PPV in a blasting operation. A three-layer ANN was found to be optimum with topology 2-5-1. Monitored and predicted PPV values were compared using coefficient of determination

(CoD) and mean absolute error (MAE). The comparison results showed that the ANN model predictions were closer to the actual values.

Mohamad et al. (2012) used artificial neural networks (ANN) to evaluate and predict blast-induced ground vibration by incorporating blast design and rock strength in the enquiry. His conclusion was that ANN method produced more accurate prediction than the empirical formula.

Monjezi et al. (2013) directed their research towards the evaluation and prediction of blast-induced ground vibration at Shur River Dam in Iran using different empirical vibration predictors and ANN model. A total of 20 blast vibration records were monitored with 16 out of them used for training of the ANN model. The remaining 4 blast vibration data sets were used for validation purposes. Performances of the different predictor models were assessed using standard statistical evaluation criteria and it was established that the ANN model is more accurate compared to the other empirical models evaluated.

Field measurements were carried out and their results were assessed to determine blast-induced ground vibrations at the Eti Mine Tülü Boron Mining Facility, Turkey by Görgülü et al. (2013). The results presented different field constants for the propagating blast vibrations depending on the direction of propagation ($K = 211.25–3,671.13$ and $\beta = 1.04–1.90$) and the damping behavior of the particle velocity. They also noticed that the field constants decrease as the rock mass rating (%) values diminish. A much higher correlation coefficient ($R\ 2 = 0.\ 95$) between the predicted and measured peak particle velocity (PPV) values was attained for artificial neural networks compared to classical evaluation methods.

2.3. BLAST-INDUCED AIRBLAST

Blast-induced airblast or overpressure is one of the negative effects of blasting operations. The resulting noise usually generates a lot of uneasiness and irritation to neighbors giving rise to complaints. Blast-induced airblast can be minimized by properly designing and implementing blasts. Blast-induced airblast is the shock wave that is refracted horizontally by density variations in the atmosphere and dies out gradually with time and distance. This pressure wave consists of audible sound and sub-audible sound.

The higher frequency portion (>15 Hz) of the pressure wave which emerges in the immediate blast premises is audible while the sub-audible is the lower frequency portion lying in the infra sound (<15 Hz) region. The sub audible portion usually occurs in the region distant from the blast site (Faramarzi et al., 2014). When an explosive charge is detonated on a flat surface, where no weather enhancement prevails, the resulting airblast overpressure levels attenuate evenly in all directions. The resulting airblast levels may be represented schematically by circular contours of decreasing intensity (Richards, 2010).

Air overpressure (AOp) waves are generally generated from four main sources:

- Air pressure pulse: displacement of the rock at bench face as the blast progresses
- Rock pressure pulse: induced by ground vibration
- Gas release pulse: escape of gases through rock fractures
- Stemming release pulse: escape of gases from the blasthole when the stemming is ejected

Air pressure pulse and rock pressure pulse are unavoidable airblast sources in bench blasting, both gases release pulse and stemming release pulse can be avoided through the blast design (Segarra et al., 2010). AOp is directly influenced by the maximum charge per delay, the distance from transducer, burden and spacing, stemming, direction of initiation and charged depth. AOp is also influenced by other parameters such as atmospheric conditions, overcharging, weak strata and conditions resulting from secondary blasting (Rodrigues et al., 2007; and Siskid et al., 1980). AOp affects structures and can result in conflict between company and those who are affected (Siskid et al., 1980; Hopler 1998; Mohanty 1998; Persson et al., 1994; Konya and Walter, 1990; and Hajihassani et al., 2014).

Seven conditions notably cause high over-pressure levels. These conditions include the following:

1. Inadequate stemming
2. Mud or weak seam venting
3. Inadequate burden confinement
4. Poor blasting timing
5. Focusing by wind or temperature inversions
6. Uncovered detonation cord

7. Overloading

2.3.1. Empirical Predictors of Airblast (AOp). Several empirical formulae and empirical curves are available in literature for the prediction of peak overpressure attenuation (Barker 2012; TM-5-855-1, 1986; Bulson, 1997).

AOp from confined blasthole charges can be obtained from the empirical equation as illustrated in Equation (2.1) (National Association of Australian State, 1983) below:

$$P = \frac{140\sqrt[3]{E/200}}{d} \tag{2.1}$$

where, P is overpressure in kPa, E is mass of charge in kg, and d is distance from center of blasthole in meter.

The air blasts or air overpressures at the blast area may be predicted using Equation (2.2) (Persson et al., 1994) below:

$$P=0.7(W^{1/3}/D) \tag{2.2}$$

where P = Air Overpressure, mbar; W = Cooperating Charge, kg; and D = Distance, m

McKenzine (1990) suggested an equation to describe the decay of overpressure as shown in Equation (2.3):

$$dB = 165\text{-}24 \log(D/W^{1/3}) \tag{2.3}$$

where, dB is the decibel reading, D is distance in meters, W is the maximum charge per delay.

The cube-root scaled distance factor (SD) is generally used to predict AOp, in the absence of monitoring. A relation connecting air overpressure and scaled distance is given below in Equation (2.4):

$$P=K\,(D/Q^{1/3})^{-\beta} \tag{2.4}$$

where, P is the Air Overpressure in linear decibels (dBL), D is the distance of measuring transducer, Q is maximum charge weight per delay, K and β are site constants, and $(D/Q^{1/3})$ is the scaled distance.

Table 2.3 gives values of site-specific constants (H and β) for different blasting conditions (Siskind et al., 1980; Hopler 1998; Hustrulid 1999; Kuzu et al., 2009)

Table 2.3. Site factors for different blasting conditions (Hajihassani et al., 2014)

Source	**Description**	**H**	**β**
USBM	Quarry blasts, behind face.	622	0.515
	Quarry blasts, direction of initiation.	19,010	1.12
	Quarry blasts, front of face.	22,182	0.966
ISEE	Confined blasts for AOp suppression.	1,906	1.1
	Blasts with average burial of the charge.	19,062	1.1
Hustrulid	Detonations in air	261.54	0.706
Kuzu et al.	Quarry blasts in competent rocks.	1833.8	0.981
	Quarry blasts in weak rocks.	21,014	1.404

Rodríguez et al. (2007) advanced a semi-empirical model for the prediction of the airwave pressure outside a tunnel due to blasting. The practical use of this method has the quantitative phase by estimating the sound levels and the qualitative phase by estimating the negative effects. Several testing proved that the approach could be used under different conditions.

Wu and Hao (2007) investigated the influence of simultaneous ground shock and airblast forces on structures. It was found that in general, airblast load governs structural response and damage when the scaled distance is small.

Kuzu et al. (2009) used site-specific scaled distances (SD) instead of conservative SD values to generate environmentally friendly and technically practicable results. They established a new empirical relationship between AOp and two parameters, the distance between blast face and the monitoring point, and the weight of explosive materials.

Rodríguez et al. (2010) reviewed the results of a previous research and pointed out that only the magnitude of the blasting airwave at the tunnel portal depends on the tunnel and blasting design parameters. Phonometric and iso-attenuation curves were proposed in order to represent the phenomenon and to synthesize the solution for a given case. For easy solutions to the problem, a charge–distance curve was proposed.

Segarra et al. (2010) investigated the propagation of airblast or pressure waves in air produced by bench blasting (i.e. detonation of the explosive in a row of blastholes, breaking the burden of rock towards the free vertical face of the block). A new AOp predictive equation based on monitoring data in two quarries was established.

2.3.2. Artificial Neural Network (ANN) Predictors of Airblast. Many investigators have applied soft computing methods like ANN, support vector machine (SVM) and fuzzy inference system to predict AOp. Khandelwal and Singh (2005) used ANN to predict air blast by incorporating the maximum charge per delay and distance between blast face to the monitoring point. The network was trained by 41 datasets with 50 epochs and tested by 15 dataset. ANN was also compared with generalized equation of air overpressure and conventional statistical relations. ANN model was the best predictor.

Mohamed (2011) predicted the AOp using fuzzy inference system and ANN. Comparison between the results of fuzzy inference system and ANN with the values obtained by regression analysis indicated that the ANN and fuzzy models have accurate prediction relative to regression analysis.

Mohamad et al. (2012) used ANN to predict AOp datasets obtained from blasting operations. Input parameters used were the hole diameter, hole depth, spacing, burden,

stemming, powder factor, and number of rows were considered. The results demonstrated the proposed model was the right choice for AOp predictions.

A new approach based on hybrid ANN and particle swarm optimization (PSO) algorithm to predict AOp in quarry blasting was investigated by hajihassani et al. (2014). AOp and some input parameters were recorded from 62 blast operations in four granite quarry sites in Malaysia. Results suggested that the PSO-based ANN model outperformed the other predictive models.

2.4. FRAGMENTATION ANALYSIS

Fragmentation analysis has been proven useful in the mining, construction and aggregate industries by helping reduce energy costs, improving efficiency and minimizing equipment maintenance costs. Mine-to-Mill optimization is the approach usually employed to accomplish the reduction of energy and cost in mining as well as processing practices. This approach involves sampling and modeling of blasting and processing, followed by computer simulation to optimize the operation and develop alternatives (Adel et al., 2006). The entire operation is taken into consideration, from blasting to comminution in order to optimize the size reduction process. Mine-to-Mill optimization has been successfully applied in gold, copper, and lead/zinc operations worldwide. As a result, the throughput increases from 5 – 18% and cost is reduced in the neighborhood of 10% (Atasoy et al., 2001; Grundstrom et al., 2001; Paley and Kojovic, 2001; Valery et al., 2001; and Adel et al., 2006).

There are several fragmentation measurement methods available. Among the methods are oversize boulder count method, sieving, visual analysis, shovel loading rate method and image analysis method. The split desktop is an example of image analysis method that is used in this research. This method usually comprises of the split software, a computer, monitor and a keyboard. The split system should also be capable of downloading the images onto the computer. To start, images are taken from muck pile or stockpile and downloaded onto a computer. The fragments in each image are delineated to determine the fragmentation of the rock fragments. Graphs of the resulting size distributions can then be plotted.

Rock fragmentation is influenced by controllable and non-controllable factors. The controllable factors include the blast design parameters and the explosive type. The non-controllable factors on the other hand are the physical and mechanical properties of the rock concerned. Certain measures should be taken to reduce the effect of these non-controllable parameters in order to attain a good rock fragmentation. Available empirical models developed have not been able to incorporate the numerous variables and their interrelations. To overcome this drawback, the Artificial Neural Network (ANN) in recent years has been put to good use.

Over the past decade, a number of research works have been executed in the area of rock fragmentation. Empirical models have been developed by earlier researchers to predict Rock fragmentation. Kuznetsov (1973) developed a relationship between mean fragment size and specific charge according to the Rosin-Rammler theory. Cunningham (1983) later improved the efficiency of this approach. These empirical methods despite their comprehensive usage failed to inculcate all the relevant input parameters necessary for the best results.

Many contemporary researchers have used artificial intelligence methods such as artificial neural network (ANN) to address effectively the weaknesses presented by these empirical methods of prediction. Monjezi et al. (2010) predicted rock fragmentation due to blasting in Sarcheshmeh copper mine using ANN. In his research, a model with architecture 9-8-5-1 trained by back propagation method was found to be optimum.

Artificial neural network (ANN) method was implemented to develop a model to predict rock fragmentation due to blasting in an iron ore mine (Bahrami et al., 2011). In developing the proposed model, eight parameters such as the hole diameter, burden, powder factor, blastability index, etc., were incorporated. Training of the model was performed by back-propagation algorithm using 220 datasets. A four-layer ANN architecture 10-9-7-1 was found to be optimum. Sensitivity analysis revealed that the most effective parameters on rock fragmentation are blastability index (G), charge per delay (J), burden (C), SMR (F) and powder factor (E).

The simultaneous prediction of rock fragmentation and backbreak in the blasting operation of Tehran Cement Company limestone mines in Iran was conducted by Sayadi et al. (2013). Back propagation neural network (BPNN) and radial basis function neural

network (RBFNN) are adopted for the simulation. In addition, regression analysis is performed between independent and dependent variables. For the BPNN modeling, a network with architecture 6-10-2 was declared optimum whereas for the RBFNN, architecture 6-36-2 with spread factor of 0.79 provides maximum prediction aptitude. Sensitivity analysis shows that inputs burden and stemming are the most effective parameters on the outputs fragmentation and backbreak, respectively.

Enayatollahi et al. (2014) did a Comparison between Neural Networks and Multiple Regression Analysis to Predict Rock Fragmentation in Open-Pit Mines. It was concluded that the ANN results possess a greater degree of accuracy, are robust, and more fault tolerant than any other analysis technique.

2.5. ARTIFICIAL NEURAL NETWORK (ANN)

Artificial neural networks have been the subject of an active field of research that has developed greatly over the past years. ANN is a computational model based on the structure and functions of biological neural networks. These networks are good at fitting non-linear functions and recognizing patterns. Hence ANN are used in mining and civil departments, military target recognition, aerospace, detection of manufacturing defects, machine monitoring and machine diagnosis, robotics, as well as Agriculture, control systems, automotive, banking, insurance, oil and gas, and telecommunications industries. Success in the mining sector is being confirmed in the areas of blast-induced ground vibration prediction, blast-produced aiblast predictions, prediction of ground fragmentation, fly rock prediction, prediction of subsidence due to underground mining and back break prediction just to mention a few.

ANNs are a form of artificial intelligence that try to mimic the actions of the human brain and nervous system. They are computational models inspired by biological neural networks, and are used to approximate functions that are generally unknown. A particular ANN has three fundamental components; transfer function, network architecture and learning law (Simpson, 1990). A typical ANN system has three layers; the input layer, the hidden layer(s) and the output layer. These three layers are interconnected and each layer consists of one or more nodes. Neurons in the input layer send data onto the hidden layer, which in turn transmit data to the output layer. ANNs

learn from data examples presented to them and use these data to adjust their weights in an attempt to capture the relationship between the historical set of model inputs and corresponding outputs. For this reason, ANNs do not need any prior knowledge about the nature of the relationship between the input/output variables (Shahin et al., 2001). Neurons can use transfer functions such as logsig, tansig or purelin to generate their outputs.

The neural network is first trained by processing a large number of datasets. Different algorithms are available for training, but backpropagation algorithm is the most proficient as it is able to accommodate large input data and able to solve problems with vast complexities. Sufficient number of experimental datasets is required to train the network. For a given set of inputs, we decide on a set of desired outputs. Using random weights, the network calculates some outputs. The calculated outputs are compared with the desired output to obtain the network error. The connecting weights are adjusted to reduce the errors in a process known as back propagation using the same learning rule. Based on the training process, a pattern is presented to the network. The new weights are calculated using equation (2.11) based on the old weights, the node input values, errors and the learning rate. This process goes on until the error is converged to a level defined by a cost function such as mean square error (MSE). Once the training phase of the model has been successfully accomplished, the performance of the trained model has to be validated using an independent testing set. Unsatisfactory network performance can be improved by retraining, increasing the number of neurons or using a larger training dataset.

The neural network after a successful training, validation and testing can be used to predict datasets outputs for given inputs based on the learning pattern. Neural network simulation often provides faster and accurate prediction compared to other methods of data analysis. Figure 2.2 demonstrates a typical ANN procedure.

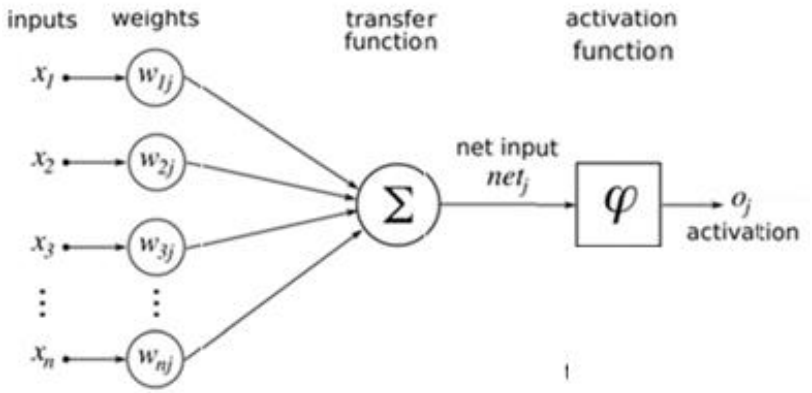

Figure 2.2. Typical ANN process

From Figure 2.2 above, a set of training data is fed through the system in a forward direction. Random weights are assigned to the data set and fed to the hidden layer in a forward direction the net input in the hidden layer is given by Equation (2.5).

The net input values in the hidden layer will be:

$$P_j = \sum_{i=1}^{n} w_{ij} x_i \tag{2.5}$$

where x_i represent the inputs, w_{ij} are the weights connecting layer i with layer j and n is the number of input units.

The net output from hidden layer is calculated using an activation function called the sigmoid function generally expressed in Equation (2.6).

$$b_j = \frac{1}{(1+e^{-P_j})} \tag{2.6}$$

The total input to layer k (the output layer) is expressed as:

$$U_k=\sum_{i=1}^{n} w_{jk}\, b_j \tag{2.7}$$

where w_{jk} is the weight connecting layer j with layer k and b_j stands for the activation of a particular function receiving neuron in layer j.

Error is generated by comparing the actual output to the desired output. The error term in a given output, k is presented in Equation (2.8):

$$\delta=d_k-a_k \tag{2.8}$$

where δ is the error term, d_k is the desired output and a_k is the actual output.

The total error function for the training pattern is given by Equation (2.9):

$$0.5\ \sum_{k=1}^{n}(d_{k-}\ a_k) \tag{2.9}$$

where d_k is the desired output and a_k is the actual output.

Changes in weights are calculated using the learning rate, the error term and the input units as illustrated in Equation (2.10).

$$\nabla W_{jk}=\eta\delta_k x_{jk} \tag{2.10}$$

where ∇W_{jk} is the change in weight, η is the learning rate, the error term is expressed as δ_k and x_{jk} is the input unit.

The calculated weight changes are then used together with the old weights to calculate new weights as shown in Equation (2.11).

$$W^N_{jk}=W_{jk}+\nabla W_{jk} \tag{2.11}$$

where the new weight is W^{N}_{jk}, W_{jk} is the old weight and ∇W_{jk} is the change in weight.

The calculated weights are then implemented throughout the network and the entire process is repeated as many epochs(cycles) as needed until the error is within the user specified goal (Khandelwal and Singh, 2009).

The first computational, trainable neural networks were developed by Rosenblatt (1958). Rosenblatt's approach was limited to solutions of linear problems. Werbos (1975) expanded the capabilities of neural networks from linear to nonlinear domains in what is known as the backpropagation algorithm. Artificial neural networks were popularized by Rumelhart and McClelland (1986).

Application of artificial neural networks in mining is growing consequently many researchers have applied the ANN system to predict blast-induced rock fragmentation, airblast and ground vibration (Khandelwal and Singh, 2005; Monjezi et al., 2010; Bahrami et al., 2011; Enayatollahi et al., 2014; hajihassani et al., 2014). ANN have also gain use in other mining and civil related works.

Maulenkamp and Grima (1999) applied neural network for the prediction of the UCS from hardness tests on rock samples based on input parameters hardness, porosity, density, grain size and rock type information of a rock sample. The results of the network were compared to predictions obtained by conventional statistical relations to examine the suitability of this technique. A dataset containing 194 rock sample records, ranging from weak sandstones to very strong granodiorites, was used to train the network with the Levenberg–Marquardt training algorithm. The conclusion was that predictions of uniaxial compressive strength by artificial neural network (ANN) were closer to the measured values.

A data mining approach to the prediction of tunnel support stability using ANN was employed by Leu et al. (2001). Rock mechanical and construction-related parameters with significant influences on support stability were filtered to train and test the ANN. It outperformed the discriminant analysis and the multiple non-linear regression method in predicting tunnel support stability.

Tawadrous (2006) used backpropagation neural network to predict the burden and spacing of the blast pattern using input parameters such as rock type, stratification, blasthole diameter, bench height, type of explosive, priming position, powder factor and

fragmentation size. He trained the network using 43 case histories collected from the various literatures and validated it with 16 cases from operational quarries. He found very high correlation for the prediction of burden and spacing by ANN.

Neaupane and Adhikari (2006) predicted ground movement around tunnels with artificial neural networks. A MATLAB® based multi-layer backpropagation neural network model was developed, trained and tested with parameters obtained from the detailed investigation of different tunnel projects published in literature. The output parameters were settlement and trough width. Diameter to depth ratio (D/Z), unit weight of soil and cohesion were among the input parameters considered for the prediction of horizontal ground movement. The neural network predicted the desired goal effectively.

Sarkar et al. (2010) reports the use of an artificial neural network to predict the deformation properties of Coal Measure rocks using dynamic wave velocity, point load index, density and slake durability index. The study confirmed that ANN is a useful tool for predicting rock strengths that are not clearly established using empirical relationships. The conclusion was that artificial neural network (ANN) is fast and cost effective.

Evaluation and prediction of the airflow rate in triaxial conditions at various confining pressures incorporating cell pressure, air inlet pressure, and air outlet pressure using ANN technique was investigated by Ranjith and Khandelwal (2012). A three-layer feed forward back propagation neural network having 3-7-1 architecture network was trained using 37 data sets measured from laboratory investigation. Based on coefficient of determination (CoD) and mean absolute error (MAE) ANN model was compared with multi-variate regression analysis (MVRA). ANN proved to be a better predictor.

Rezaei et al. (2012) developed an ANN model to predict burden in the blasting operation of Mouteh gold mine, using geomechanical properties of rocks as input parameters. Blastability index (BI), rock quality designation (RQD), unconfined compressive strength (UCS), density, and cohesive strength were among the input parameters used. It was observed that the ANN prediction capability is better than that of MVRA. Further, a sensitivity analysis shows that while BI and RQD were the most sensitive parameters, cohesive strength was considered as the least sensitive input parameters on the ANN model output.

Monjezi et al. (2013) applied ANN method to predict the flyrock in the blasting operations of Sungun copper mine, Iran. Architecture 9-5-2-1 was found to be optimum after training with back-propagation algorithm. Flyrock were also computed from various available empirical and statistical models. ANN was then compared with the statistical and empirical methods for superiority in prediction capabilities. Comparison of the results showed absolute superiority of the ANN modeling over the empirical, as well as, statistical models. It was also observed that the powder factor, hole diameter, stemming and charge per delay are the most effective parameters on the flyrock.

Monjezi et al. (2013) utilized artificial neural networks (ANNs) for predicting backbreak in the blasting operation of the Chadormalu iron mine (Iran). After trying various hidden layers and neurons, network with topology 10-7-7-1 was deemed optimum. ANN model proved superior over the conventional regression analysis using Mean Square Error (MSE), Variance Account for (VAF) and coefficient of determination (R^2) as the means of comparison. Sensitivity analysis revealed that burden is the most influencing parameter on the backbreak, whereas water content is the least effective parameter in the research.

Majdi and Rezaei (2013) developed an ANN and multivariable regression analysis (MVRA) models in order to predict Uniaxial Compressive Strength (UCS) of rock surrounding a roadway. Rock type, Schmidt hardness, density and porosity were the input parameters and UCS the output parameter used for the study. It was concluded that performance of the ANN model is considerably better than the MVRA model with rock density and Schmidt hardness being the most effective input parameters.

ANN was used to predict backbreak in blasting operation of the Sangan iron mine, Iran by Monjezi et al. (2014). Network with two hidden layers was found to be optimum after trying different types of networks. Predictions by the ANN model demonstrated a higher correlation (R^2 = 0.868) and lesser error (RMSE = 0.495) compared to the regression model. Rock factor was the most sensitive and number of rows was the least sensitive parameter on the back break.

Trivedi et al. (2014) focused on predicting the distance covered by the flyrock induced by blasting using artificial neural network (ANN) and multi-variate regression analysis (MVRA). Blast design and geotechnical parameters, such as linear charge

concentration, burden, stemming length, specific charge, unconfined compressive strength (UCS), and rock quality designation (RQD) were used as input parameters and flyrock distance used as output parameter. Comparison of predicted results by ANN and MVRA showed that Back propagation neural network (BPNN) has been proven to be a superior predictive tool when compared with MVRA.

2.6. SUMMARY

Numerous empirical and artificial neural network (ANN) predictors are available in literature to help predict ground vibration, airblast and rock fragmentation. Empirical equations for predicting ground vibration and airblast are based on the maximum charge per delay and the distance from blast face to monitoring point. These empirical equations are unable to concurrently predict more than one output and are restricted to just two input parameters. To address the above weaknesses of empirical predictors, ANN models have been used. ANN models have the ability to consider all relevant input parameters and more than one output can be predicted using ANN models. The methodology of the research is captured in section 3.

3. METHODOLOGY

Input and output data needed for the exercise were extracted from the blast records of the mining company spanning a three-year period. Seven input and three output parameters were used for the ANN processing. The inputs considered for the research are those that are most sensitive to the outputs from literature. The inputs are inter-related, i.e. changing one parameter affects the other. The inputs are maximum charge per delay, distance from blast to monitoring point, hole depth, stemming length, hole diameter, powder factor and spacing to burden ratio. The output parameters on the other hand are rock fragmentation, ground vibration and airblast. These inputs and outputs are fed into a MATLAB-based ANN system to establish an optimum model. The optimum model generated is applied to series of blasts with the view to optimizing the fragmentation while minimizing the ground vibration and airblast.

3.1. DATA COLLECTION

Ground vibrations and airblasts were recorded using Minimate Plus Base Unit configured with triaxial geophones and Linear Microphones (2-250Hz). This instrument was chosen because of its flexibility, reliability and ease of use. Prior to blasting, the microphone and geophone are connected to the unit and located at selected points in blast catchment areas. The setup is placed firmly on a strong and levelled ground to allow accurate and reliable readings. The unit is turned on and the sensors are checked to make sure they are in good state and functional. Trigger level is set and the instrument begins recording automatically when the trigger level is exceeded. Recording stops after blasting when readings fall below the trigger level. The geophone measure ground vibrations while the sound pressure (airblast) is measured by the microphone. After blasting, the unit is taken to the office and the results downloaded onto the computer for further analysis. Fragmentation analysis is then conducted on blasted material using split technology.

Fragmentation analysis allows the quantification and size estimation of the fragmented ore, and provides a size distribution of rocks by taking sample images from a muck pile, a truck tipper or a conveyor belt. Knowledge of results from such analysis is

used to predict the fragmentation outputs of subsequent blasts in a comparable geological area. Rock fragmentation begins with the drilling and blasting process.

Drilling is done by Sandvik DP1500 hydraulic rigs. Blast holes diameters of 115 mm are drilled vertically with staggered drill-hole pattern to different depths (5m, 7.5m and 10m). Priming is carried out using non-electric (NONEL) detonators and pentolite cartridges. Drilled holes are checked for correct depths and filled with ANFO (P100 bulk emulsion) of average density 1.13 g/cm^3. The holes are then stemmed with appropriately sized gravels. The inter hole delays are 17ms or 25ms and the inter row delays are 42ms or 67ms. Averagely 50 to 300 holes are blasted in a round.

Split digital technology was used for the particle size distribution examination. This technology was adapted because it is more economical and accurate compared to other techniques. After blasting, an excavator spreads the muck pile to create a wider surface area and quality images of blasted material taken. The images from muck piles are uploaded unto a computer equipped with the split digital technology and particle sizes analyzed. Particle sizes falling within 0.1m – 0.9m are considered to be in range, below 0.1m are undersize and above 0.9m deemed oversized. Percentages passing through the in-range category were used to represent fragmentation. Figures 3.1 and 3.2 are the sample image, and size distribution curve respectively.

Figure 3.1. Image prepared for fragmentation analysis

A grid system size 0.2m is superimposed on the sample image to ascertain the individual particle sizes as indicated in Figure 3.1 above. Figure 3.2 shows the particle size distribution curve generated based on the percentage of rock particle sizes passsing through the mesh. The Majority of the particle sizes for this particular sample were within the range of 0.1 to 0.9m.

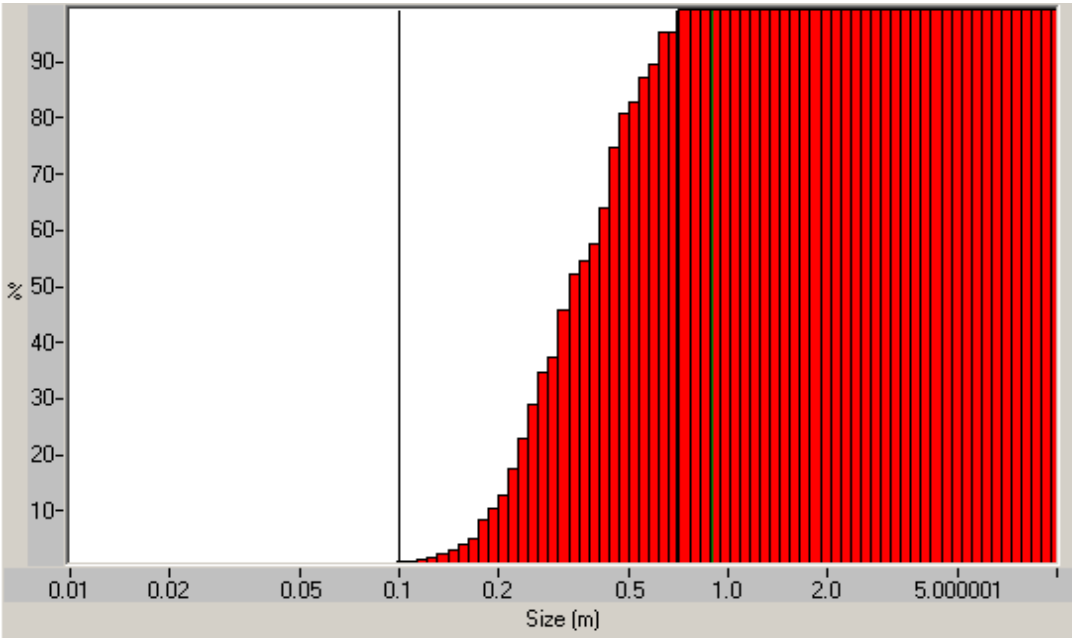

Figure 3.2. Particle size distribution curve

3.2. INPUT AND OUTPUT DATA SETS

A Total of 180 different blast data taken from the mine was used for the ANN analysis. The input parameters used for the experiment are (i) Maximum charge per delay, (ii) Distance from blast to monitoring point, (iii) Hole depth, (iv) Stemming length, (v) Hole diameter, (vi) Powder factor and (vii) Spacing to burden ratio. Among several parameters, the seven (7) chosen inputs parameters are those known from literature to significantly influence the rock fragmentation, ground vibration and airblast. Thus, the

analysis for the experiment was carried out with the seven input parameters and their corresponding outputs for the 180 different blast data sets. These inputs are enumerated in Table 3.1 as follows.

Table 3.1. Input parameters and their ranges

Parameter	**Symbol**	**Range**
Charge per delay (kg)	Q	30 - 105
Distance from blast to monitoring point (m)	D	700 - 2,529
Hole depth (m)	H	3 - 10.8
Stemming length (m)	L	1.0 - 4.0
Hole diameter (mm)	T	115 - 140
Powder factor (kg/m^3)	P	0.3 - 1.0
Spacing to burden ratio	B	0.95 – 1.22

The range of corresponding output parameters (i.e. rock fragmentation, ground vibration and airblast) are also captured in Table 3.2.

Table 3.2. Output parameters and their ranges

Parameter	**Symbol**	**Range**
Rock fragmentation (%)	A	65 - 95
Ground vibration (PPV),mm/s	C	0.13 – 0.95
Airblast (Air Overpressures), dBL	K	76 - 123

From Table 3.2, rock fragmentation is represented by the percentage of particle sizes that are within 0.1m to 0.9m range. The Peak Particle Velocity (PPV) and Air Overpressure (AOp) respectively quantify ground vibration and airblast.

3.3. ARTIFICIAL NEURAL NETWORK (ANN) ARCHITECTURE

A three-layer, defined by an input layer, a hidden layer and an output layer feed-forward back-propagation neural network was developed. This three-layer neural network is used to predict rock fragmentation, ground vibration and airblast due to its ability to accommodate large input data and its capabilities to solve problems with vast complexities. The term "feed-forward back-propagation" indicates a forward activation flow of inputs and the backwards error propagation of weight adjustments. The artificial neural network (ANN) model was generated by (i) importing blast data in csv format into MATLAB® (ii) creating network using nntool function (iii) training, validation and testing.

A total of 180 data sets were used for the study. The data was divided into training (70%), testing (15%) and data validation (15%). The data was then imported to MATLAB® and network formed using the nntool function. NNTOOL opens the Network window, which allows you to import, create, use, and export neural networks and data. The network type selected for the training was feed-forward back-propagation because it is good for non-linear fittings. Trainlm was the training function adopted because it is the fastest backpropagation algorithm in the toolbox. Trainlm function updates weight and bias values according to Levenberg-Marquardt optimization. The learning functionality used was the Learngdm and this function takes several inputs. Learngdm is the gradient descent with momentum weight and bias learning function. The performance function e.g. Mean square error (MSE), the number of layers, the number of neutrons and the transfer function e.g. tansig are all selected accordingly in order to create the network. After successfully creating a network, the next step is to train the network. Figures 3.3 and 3.4 are examples of ANN network window and ANN network architecture respectively.

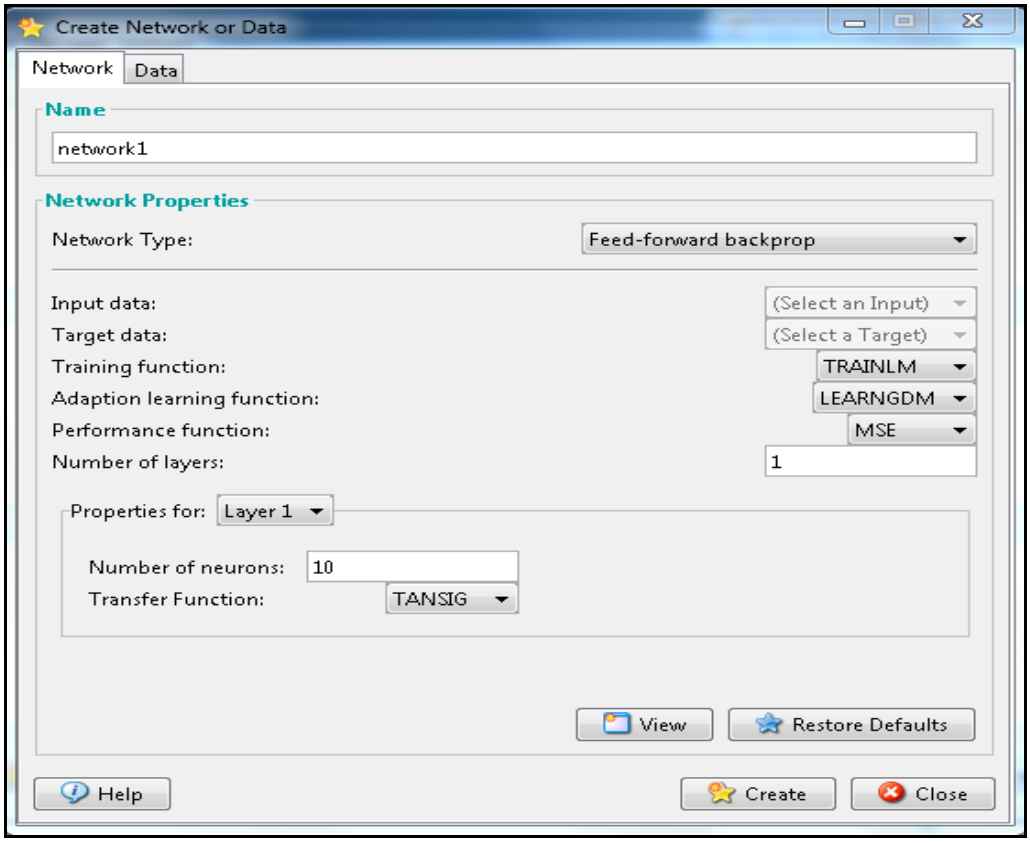

Figure 3.3. Typical ANN network window

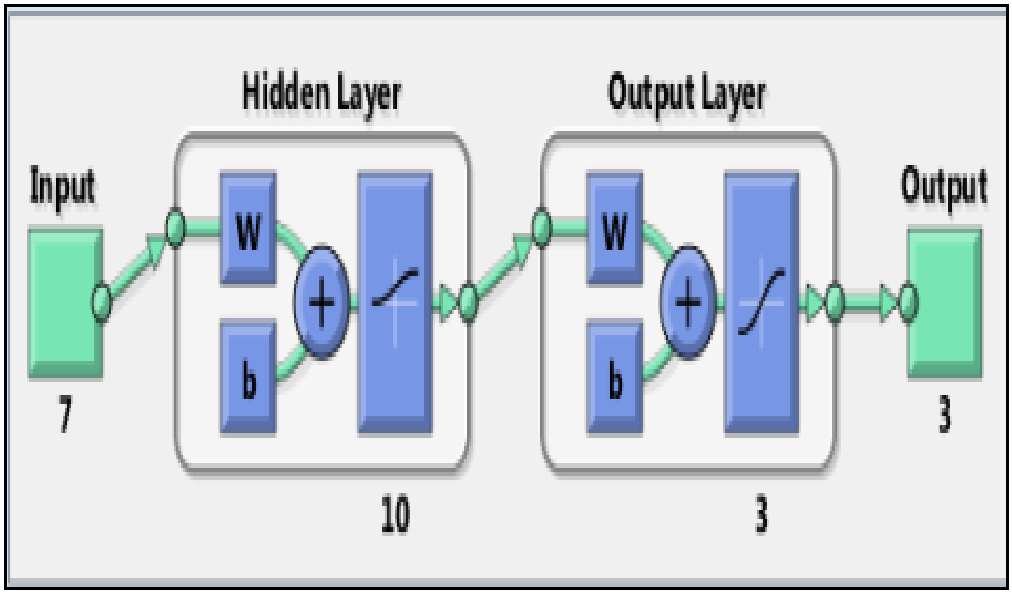

Figure 3.4. Typical ANN network architecture

Training of the network was performed using the Levenberg-Marquardt backpropagation algorithm as it is very fast. For the given set of inputs, a set of targets are decided. Using the random weights, the network calculates some outputs using transfer functions (i.e. tansig and logsig). The calculated outputs are compared with the targets to obtain the network error. The connecting weights are adjusted to reduce the errors using the same learning rule. Based on the training process, a pattern is presented to the network. The new weights are calculated using Equation (2.11) based on the old weights, the node input values, errors and the learning rate. This iterative process is repeated until the error is below a specified value/level. Validation and testing are conducted to estimate the accuracy of the network/model.

After a successful training, validation and testing using different network architectures, the optimum network architecture is chosen. A comparison is carried out for the different network architectures created as indicated in Table 3.3 using the coefficient of determination (R^2) and the root mean square error (RMSE), network with architecture 7-13-3 (i.e. seven neurons in input layer, thirteen neurons in hidden layer and three neurons in the output layer) was deemed optimum because it had the least RMSE.

Equation (3.1) (Pearson et al. 1995; Neaupane and Adhikari 2006; Enayatollahi et al., 2014) below was used in computing the root mean square error (RMSE) for the various models presented in Table 3.3.

$$\text{RMSE}= \sqrt{\frac{\sum_{i=1}^{N}(ypred,i-ymeas,i)^2}{N}} \tag{3.1}$$

where, y_{pred}, y_{meas}, and N represent the predicted output, measured output, and the number of input–output data pairs, respectively.

Table 3.3. Comparison of different network architectures

Model	Transfer function	Number of Neurons	RMSE	R^2
1	tansig	8	0.418	0.99953
2	tansig	10	0.556	0.99958
3	tansig	13	0.307	0.99963
4	tansig	18	0.535	0.99924
5	logsig	8	0.354	0.99934
6	logsig	10	0.711	0.99953
7	logsig	12	0.982	0.99948

Notice in Table 3.3 above, model 3 with network architecture 7-13-3 has the lowest RMSE, thus it is considered the optimum predictive model. The training, validation and testing curves for the different artificial neural network (ANN) models are detailed in Appendixes A and B.

The optimum network architecture and regression curves are illustrated in Figures 3.5 and 3.6 respectively.

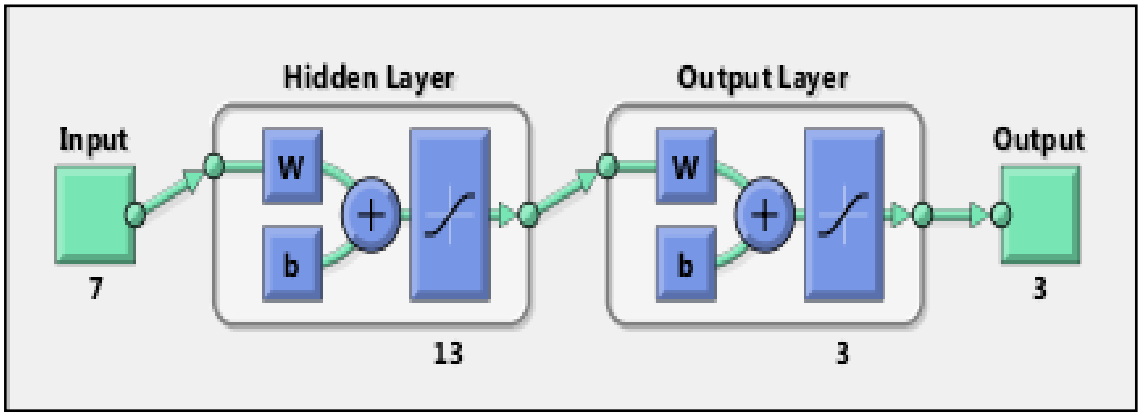

Figure 3.5. Optimum network architecture

Figure 3.5, represents the optimum network architecture with seven (7) neurons in the input layer, thirteen (13) neurons in the hidden layer and three (3) neurons contained in the output layer as already discussed.

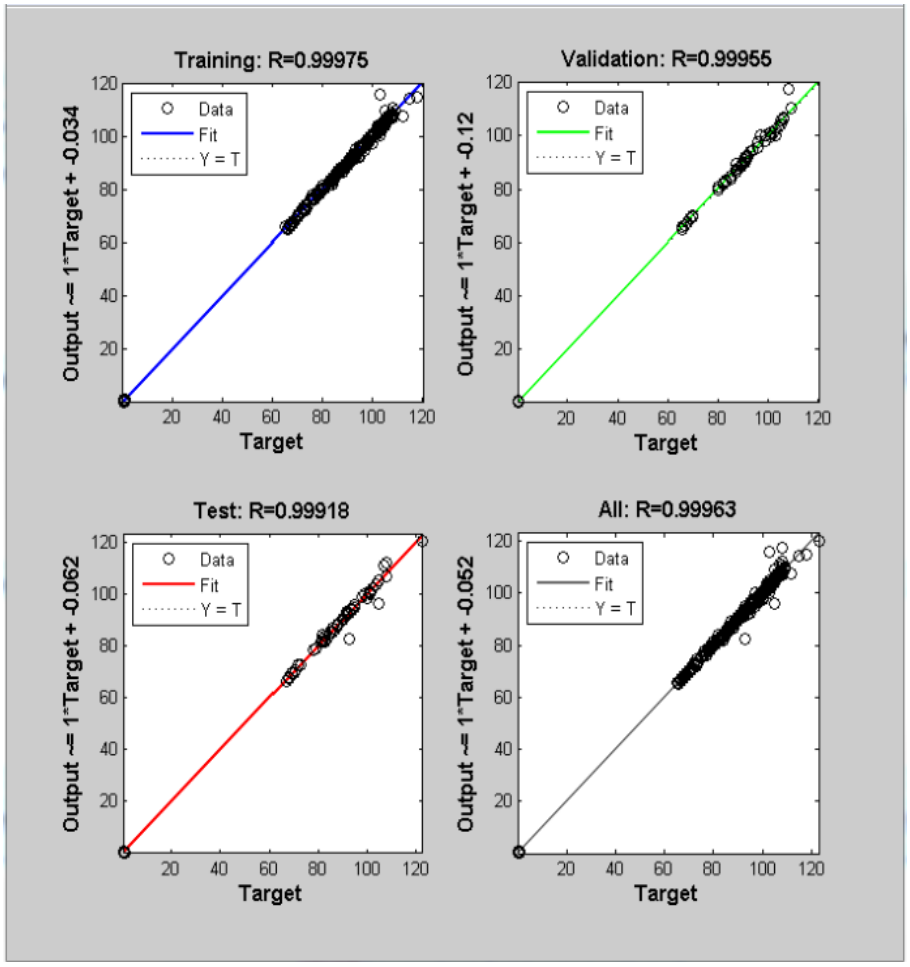

Figure 3.6. Optimum network regression curves

Figure 3.6 above represents a regression curve showing the relationship between the outputs and targets for training, validation and testing stages. There is an excellent correlation between the output and target datasets for the training, validation and testing stages. Therefore, the combined curve demonstrates a strong relationship between the

output and the target considering the R^2.The regression curves, performance graphs and training plots for the different ANN models tested are listed in Appendixes A and B.

The optimum network developed was then used to predict thirty (30) new data sets with known outputs as illustrated in Table 3.4. Results of the predictions were then compared with the known outputs to estimate the accuracy of the optimum model.

Figures 3.7, 3.8 and 3.9 are graphs comparing the predicted and measured PPVs, AOps and rock fragmentations respectively.

Table 3.4. Measured and predicted outputs

Measured PPV (mm/s)	Predicted PPV (mm/s)	Measured AOp(dBL)	Predicted AOp(dBL)	Measured Fragmentation (%)	Predicted Fragmentation(%)
0.33	0.31	102	102.3	86	85.6
0.26	0.26	101	101.2	69	69.1
0.26	0.26	100	100.2	70	69.5
0.3	0.28	102	101.9	68	67.7
0.27	0.27	93	93.2	69	68.6
0.28	0.26	101	101.0	66	66.1
0.28	0.26	102	101.9	66	66.1
0.32	0.30	100	100.4	78	77.5
0.26	0.28	90	89.9	79	78.8
0.27	0.28	94	93.9	83	82.7
0.27	0.28	95	95.0	82	82.4
0.26	0.28	92	92.3	83	83.1
0.26	0.28	93	93.4	83	82.8
0.27	0.27	100	100.2	78	78.2
0.26	0.27	96	95.7	82	81.9
0.75	0.71	85	85.3	93	92.3
0.26	0.26	99	98.9	71	70.6
0.26	0.26	100	99.7	70	70.3
0.27	0.27	98	98.5	78	78.2
0.29	0.32	96	95.8	91	91.0
0.29	0.32	96	96.5	91	92.9
0.39	0.40	106	106.0	91	91.1
0.27	0.27	100	100.2	74	73.8
0.25	0.27	95	95.0	76	76.6
0.36	0.35	102	101.7	90	90.3
0.29	0.33	92	92.1	91	90.8
0.31	0.30	98	97.8	84	84.0
0.3	0.30	96	96.4	84	84.2
0.56	0.55	109	108.3	89	89.2
0.46	0.49	103	103.4	90	89.7

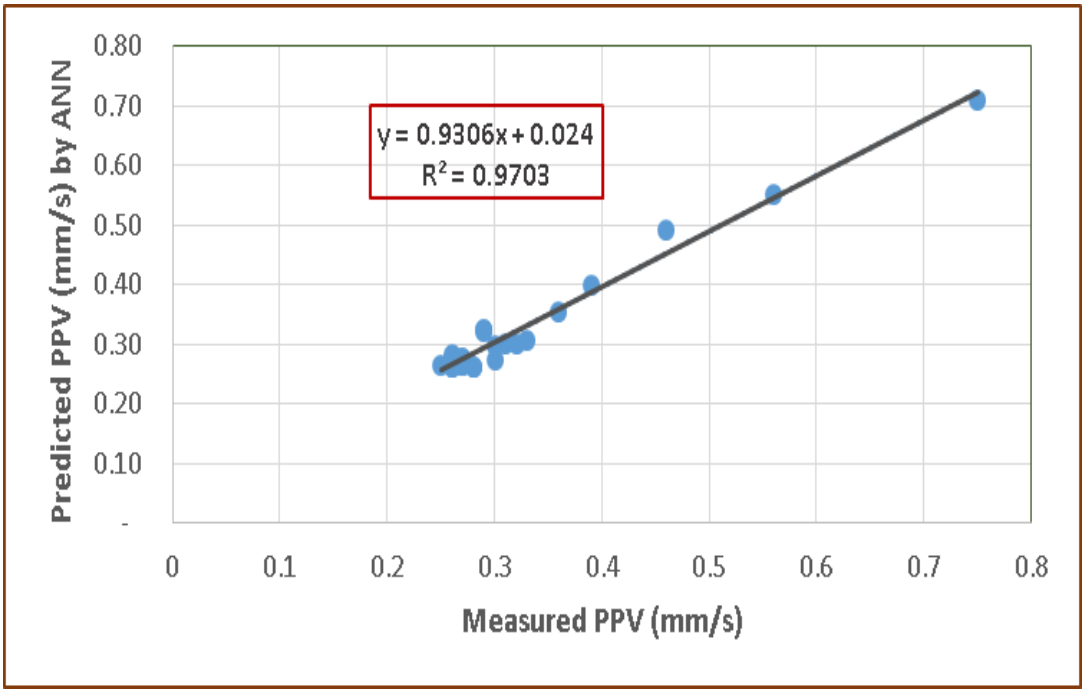

Figure 3.7. Relation between predicted and measured PPV by ANN

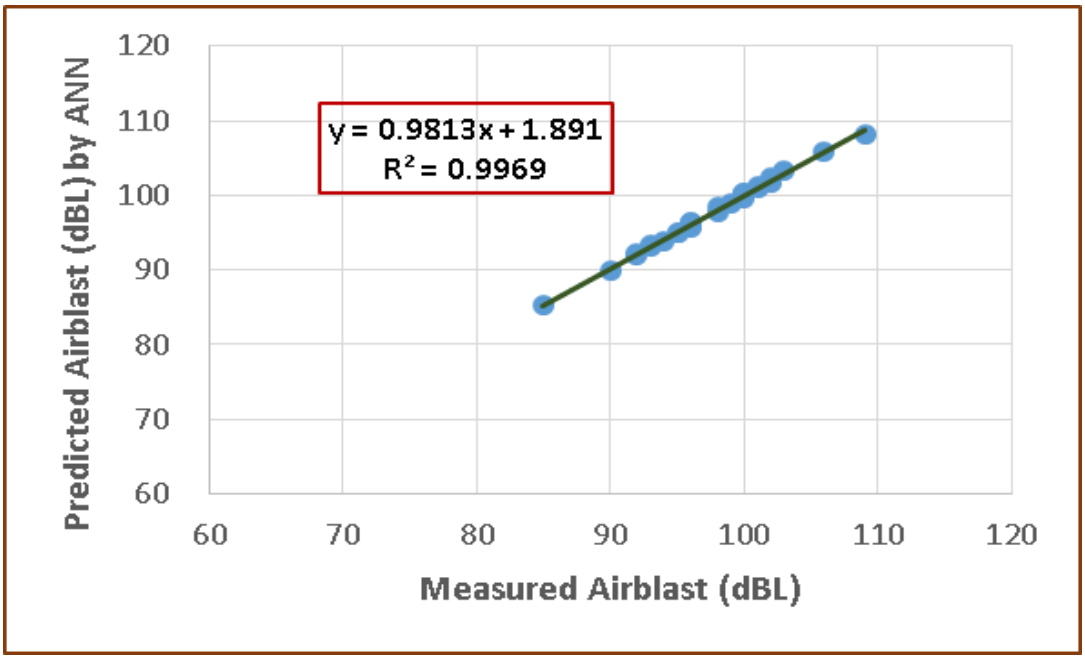

Figure 3.8. Relation between Predicted and Measured Airblast by ANN

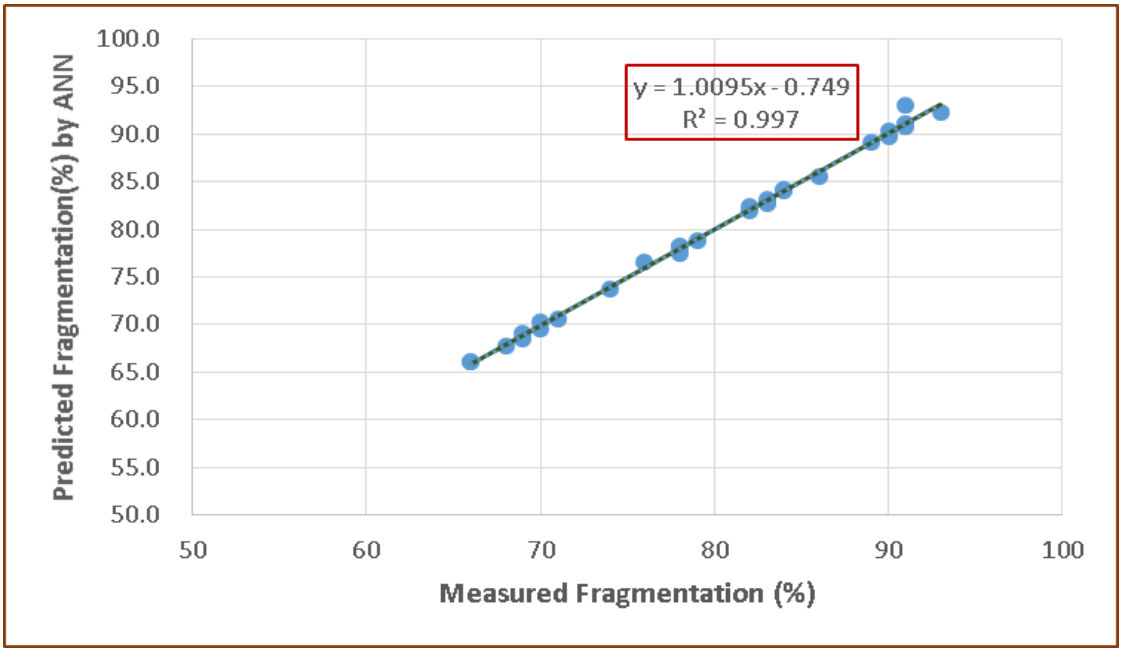

Figure 3.9. Relation between predicted and measured fragmentation by ANN

The coefficient of determination (R^2) for Figures 3.7, 3.8 and 3.9 above are very close to one (1) indicating a strong correlation between the predicted and measured values for the output parameters using the optimum artificial neural network (ANN) tool. A strong correlation between the predicted and measured outputs show that the optimum ANN model predicts the actual physical field behavior thus the ANN model can be used to predict outputs in the field based on known input data set.

3.4. REGRESSION ANALYSIS

Multivariate regression analysis (MVRA) predictors have the ability to predict outputs given multiple inputs. Multivariate regression analysis (MVRA) was developed using the same input-independent variables and output-dependent variables used for the ANN processing. Using the MVRA tool, a variable (dependent variable) is predicted using known values (independent variables).

In general, the multiple regression equation of $\hat{z}$ on X_1, X_2, …, X_k is given by:

$$\hat{z} = b_0 + b_1 X_1 + b_2 X_2 + \ldots\ldots\ldots\ldots\ldots\ldots + b_k X_k \quad (3.2)$$

where the term $\hat{z}$ is the predicted value estimated from X_i, b_0 is the intercept, and bi are the partial regression coefficients. The coefficient of determination (R^2) is usually used to test the predictive ability of a multiple regression equation. A closer value of R^2 to unity implies an accurate predictive model. The multiple regression presents two different overlaps: the overlap for the combined effect and the overlap for the individual effect (Enayatollahi et al., 2014).

Based on Equation (3.2) above, equivalent equations are derived relating rock fragmentation, ground vibration (PPV) and airblast (AOp) to their respective input parameters. The multiple regression equations for the various outputs are defined as follows:

Ground vibration (mm/s) = 0.0002[D]+0.0080[Q]-0.0561[H]-
0.5604[B]+0.0070[T]+0.0667[P]+0.0511[L]-0.3705 (3.3)

Airblast(dBl) = 0.0174[D]+0.0126[Q]-0.4164[H]+28.2977[B]-0.2298[T]- 23.4536[P]–
0.5281[L]+93.2605 (3.4)

Fragmentation (%) = 0.0009[D]-0.1718[Q]+0.0317[H]-29.2185[B]-0.0366[T] –
70.1293[P]+3.3022[L]+156.8241 (3.5)

Parameters in Equations (3.3), (3.4) and (3.5) are defined in Table 3.3.

The multiple regression model generated was also used to predict ground vibrations, airblast and rock fragmentation using the same thirty (30) data set used for the ANN analysis previously. Results of the predictions were compared to measured outcomes for correlation. Figures 3.10, 3.11 and 3.12 illustrate the relationship between predicted and measured PPV, AOp and rock fragmentation respectively using multivariate regression analysis (MVRA).

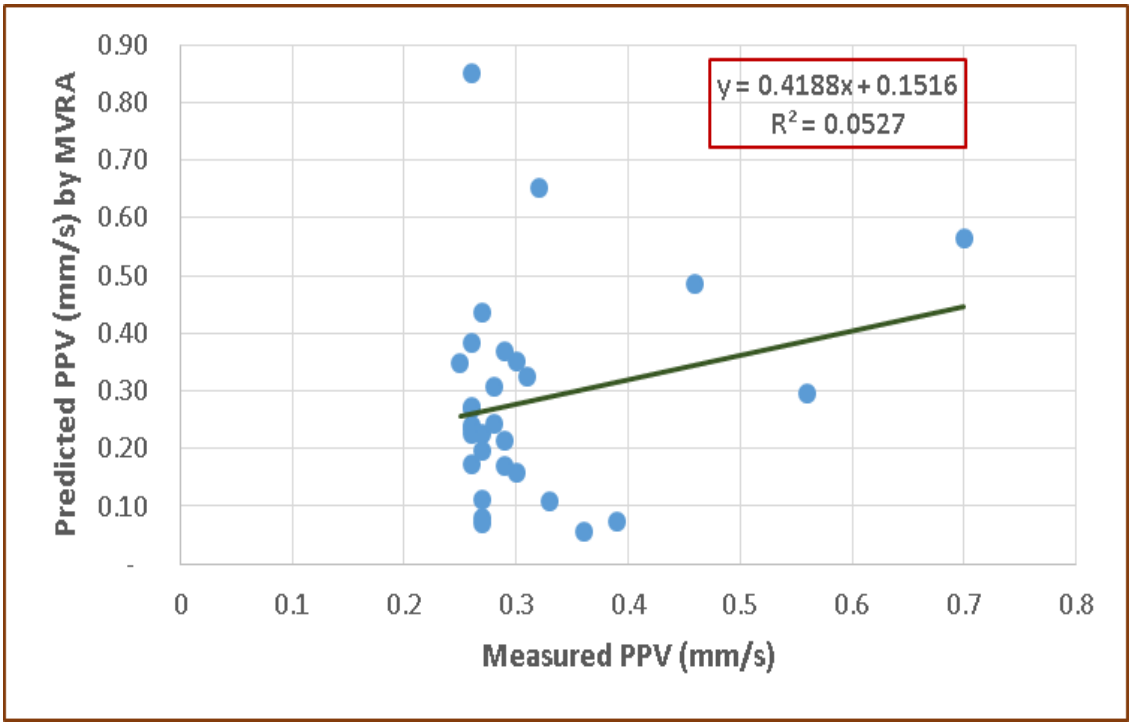

Figure 3.10. Relation between predicted and measured PPV by MVRA

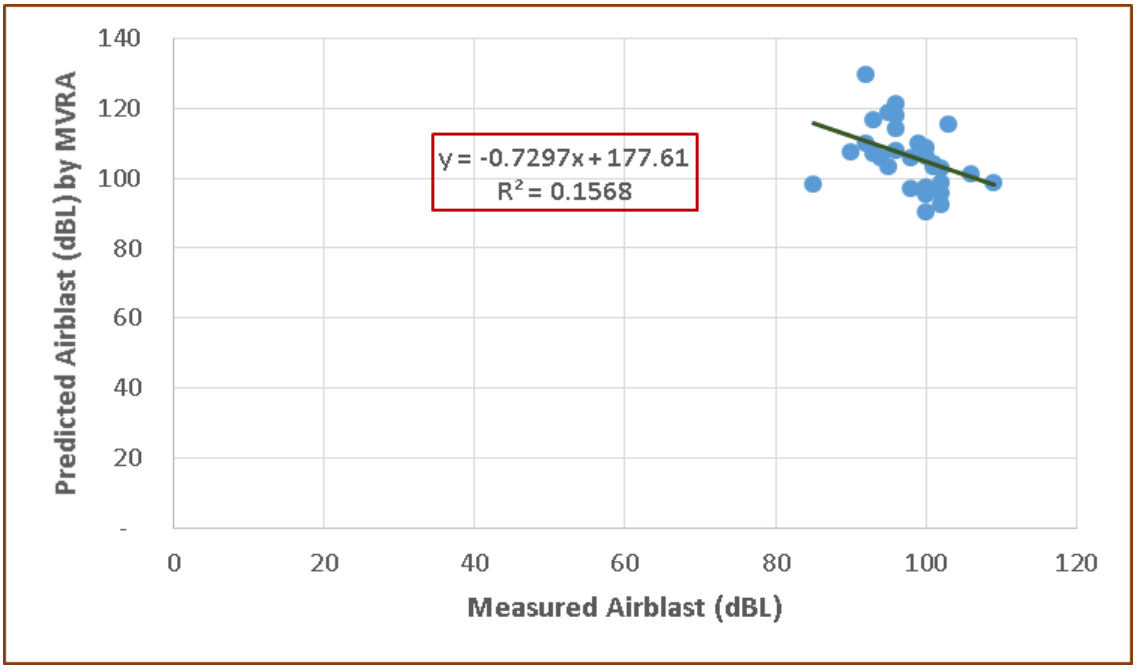

Figure 3.11 Relation between predicted and measured airblast by MVRA

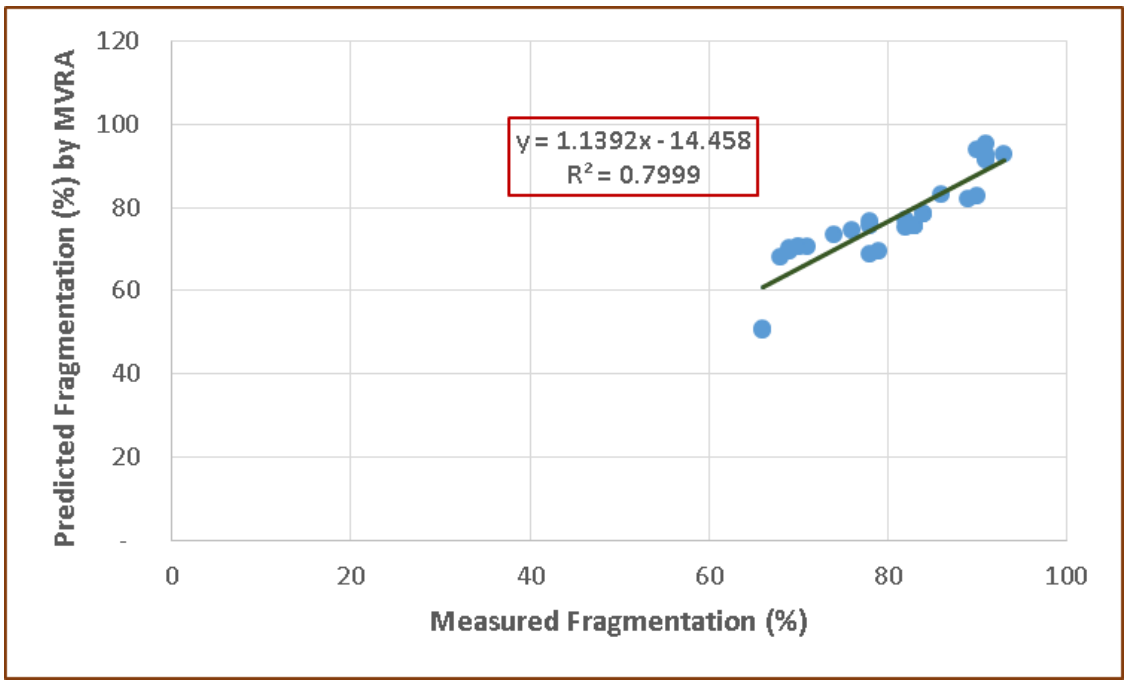

Figure 3.12. Relation between predicted and measured fragmentation by MVR

Predictions made using the MVRA tool were mostly poor as demonstrated by Figures 3.10, 3.11 and 3.12 with the strongest relationship occurring for comparison between the predicted and measured fragmentation in Figure 3.10. The weak correlation is because the MVRA tool is not able to account for the inherent complexities in the input parameters, hence the need for the ANN model.

3.5. EMPIRICAL PREDICTORS FOR GROUND VIBRATION (PPV)

Various researchers proposed different equations for the prediction of PPV such as Duvall and Fogelson (1962), Langefors and Kihlström (1963), Ambraseys and Hendron (1968), Bureau of Indian Standards, BIS (1973). These predictor equations are summarized in Table 3.5. The blasts are scaled to equivalent distances using the maximum charge per delay and distance from blast to monitoring point. The equations are generally non-linear but can be expressed in linear by logarithmic transformation of variables. The site-specific constants (K and B) are generated by plotting the log

transformed PPV against the log transformed scaled distances. Figures 3.13, 3.14, 3.15, and 3.16 illustrate the square-root-scaled distance and PPV on log–log scale. The different empirical predictors are presented in Table 3.5.

Table 3.5. Predictor equations

Names	Equation
USBM (1959)	$V=K[R/Q_{max}]^{-B}$
Langefors–Kihlstrom (1963)	$V=K[(Q_{max}/^{R2/3})1/2]^{B}$
Ambraseys–Hendron (1968)	$v = K[R/(Q_{max})^{1/3}]^{-B}$
Bureau of Indian Standard (1973)	$v = K[(Q_{max}/R^{2/3})]^{B}$

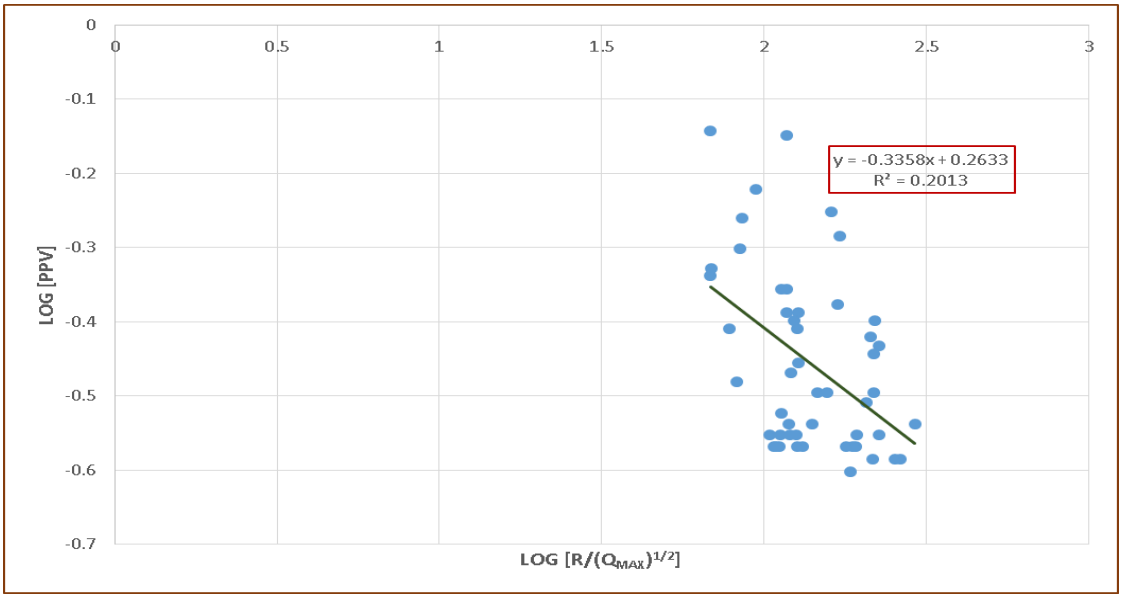

Figure 3.13. PPV and Scaled distance on log–log scale for USBM

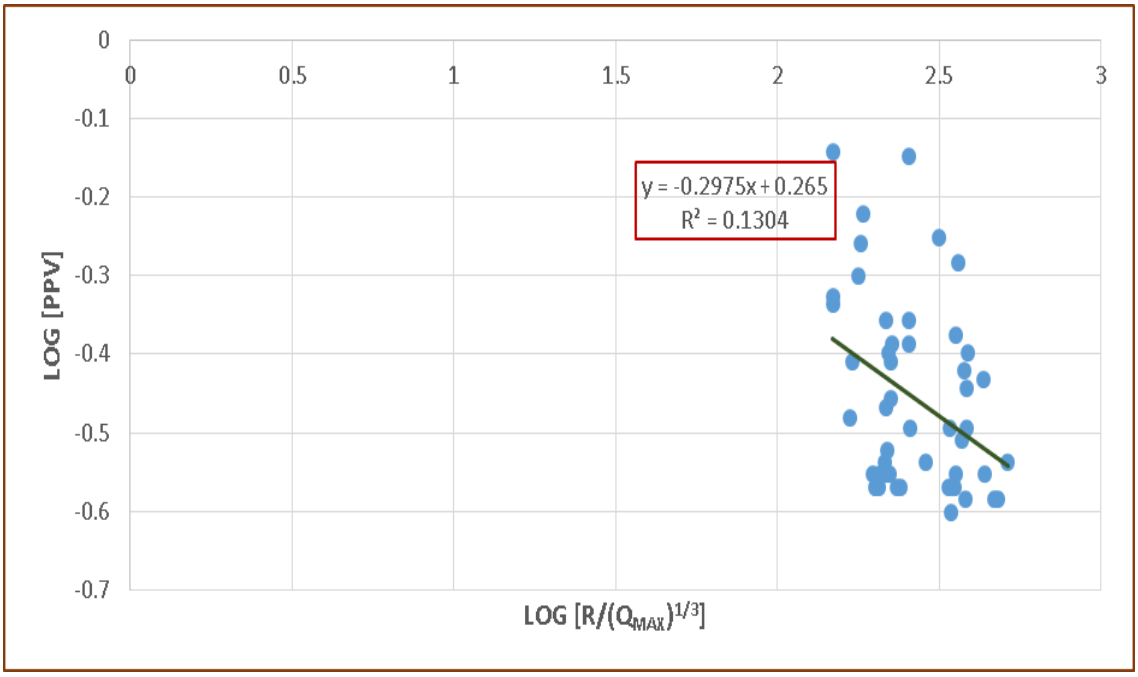

Figure 3.14. PPV and Scaled Distance on log–log scale for Ambrasey-Hendron

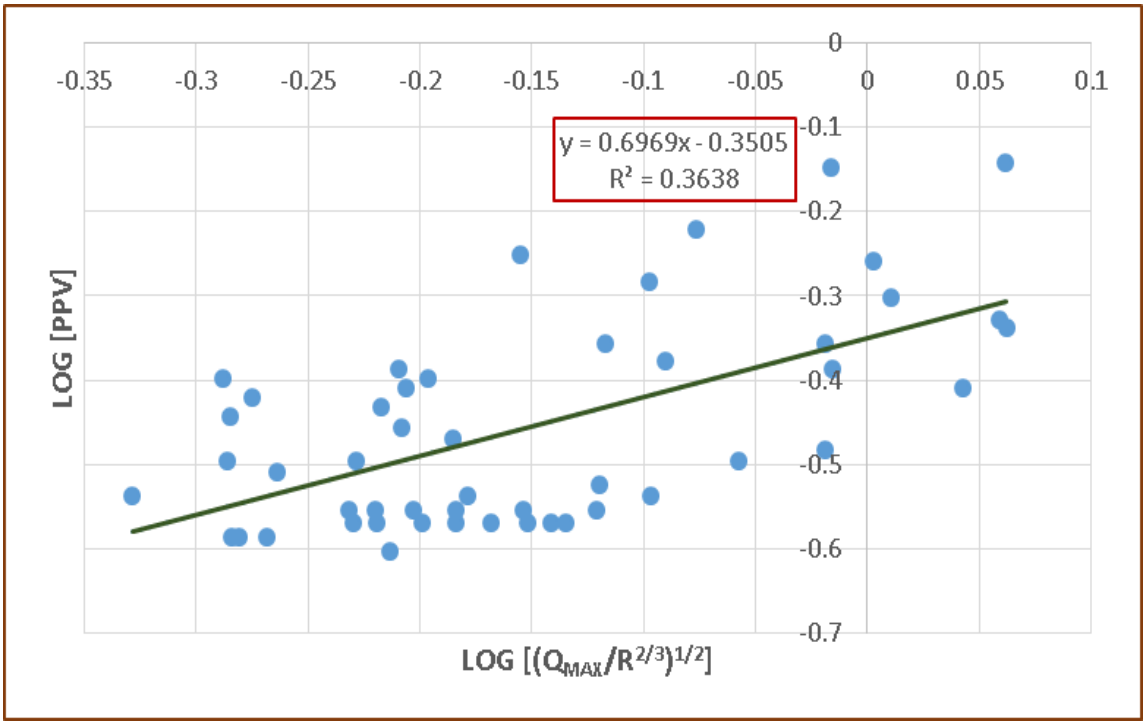

Figure 3.15. PPV and Scaled Distance on log–log scale for Langefors–Kihlstrom

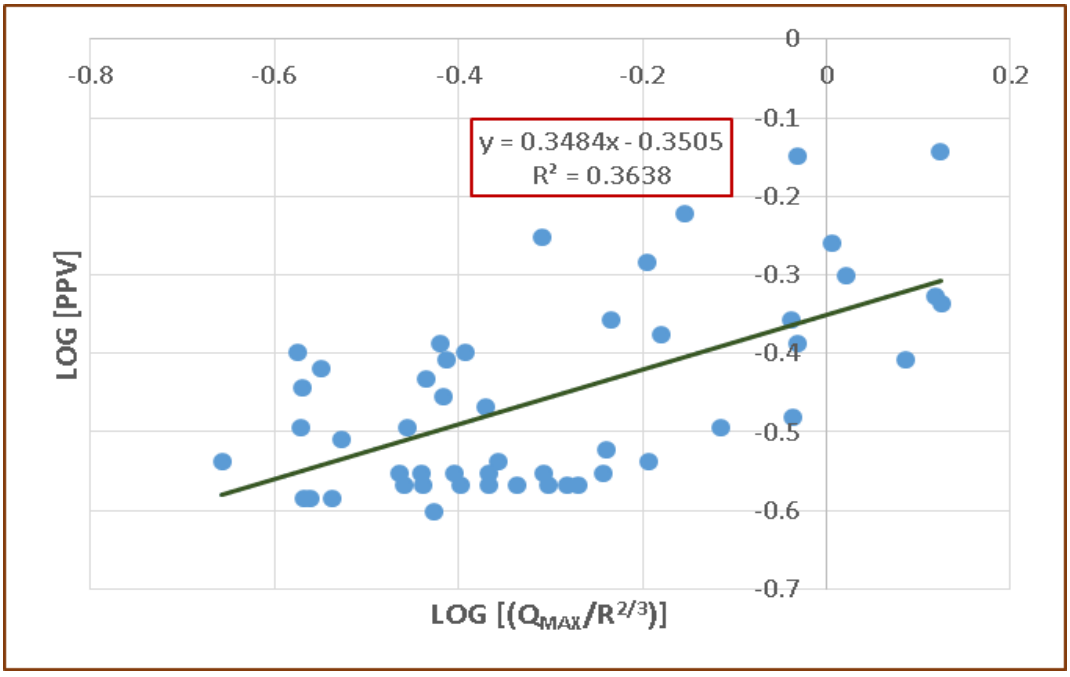

Figure 3.16. PPV and scaled distance on log–log scale for Indian standard predictors

The connection between PPV and scaled distance is established in Figures, 3.13, 3.14, 3.15 and 3.16 above using empirical predictors. The above graphs generally indicate a weak link between PPV and scaled distance as shown by the relatively smaller R^2 values.

Table 3.6 represents the site constants for the different empirical predictors derived from the plots above.

Table 3.6. Calculated values of site constants

PREDICTORS	**SITE CONSTANT**	
	K	B
USBM	1.834	-0.336
AMBRASEY-HENDRON	1.841	-0.298
LANGEFORS–KIHLSTROM	0.446	0.697
INDIAN STANDARD PREDICTORS	0.446	0.348

The empirical equations have been utilized for the prediction of PPV using 30 data sets. Figures 3.17, 3.18, 3.19 and 3.20 highlight the measured and predicted PPV by the different predictor equations.

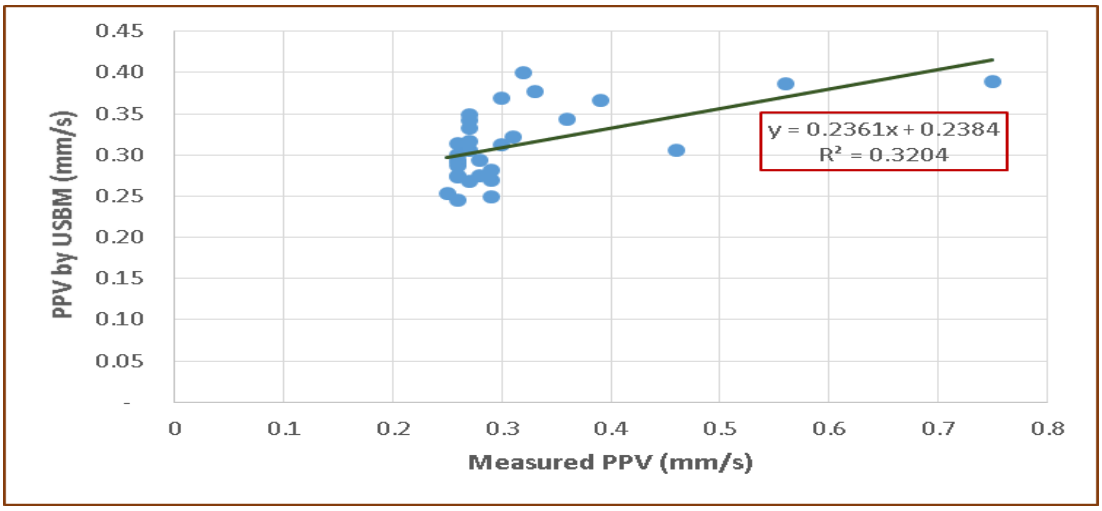

Figure 3.17. Measured and predicted PPV by USBM Equation

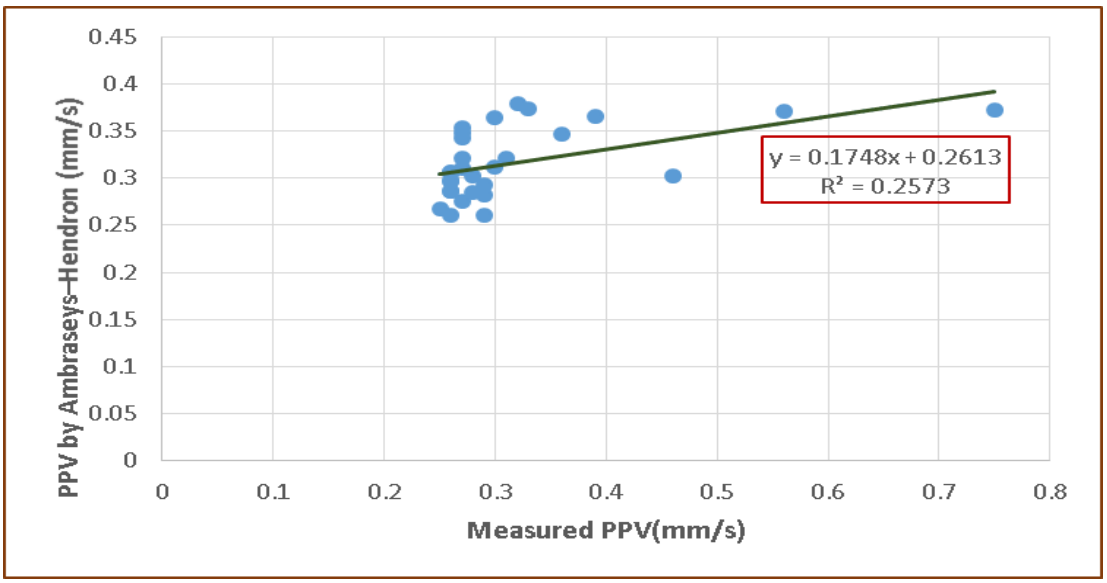

Figure 3.18. Measured and predicted PPV by Ambraseys–Hendron equation

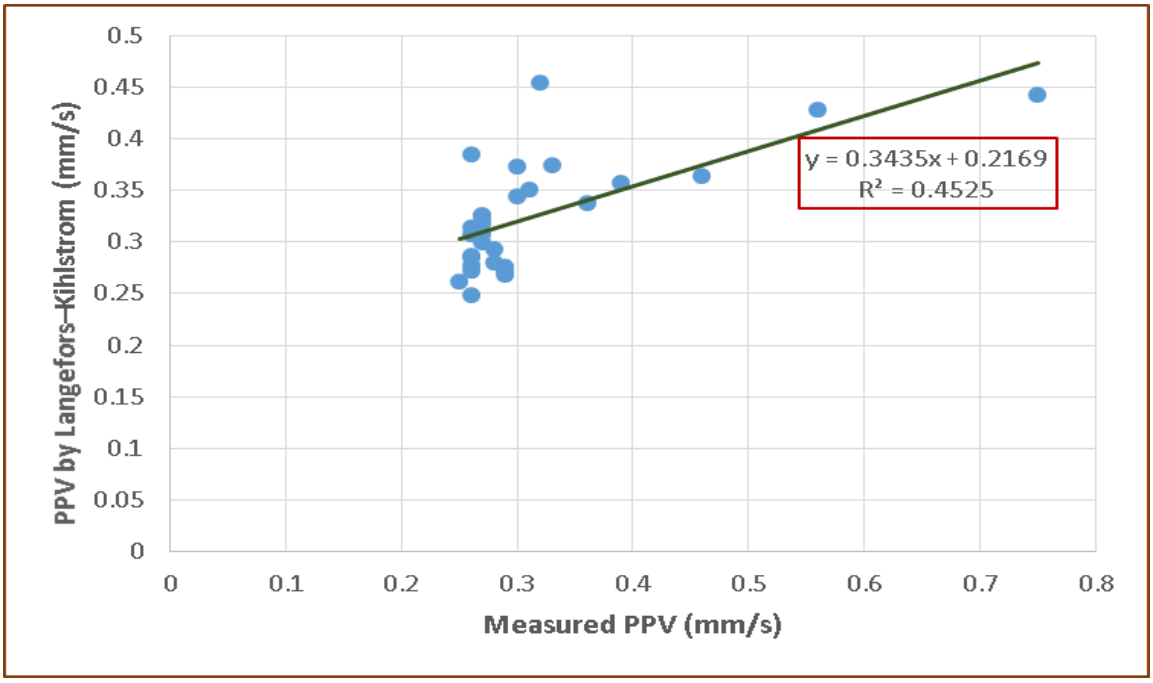

Figure 3.19. Measured and Predicted PPV by Langefors–Kihlstrom equation

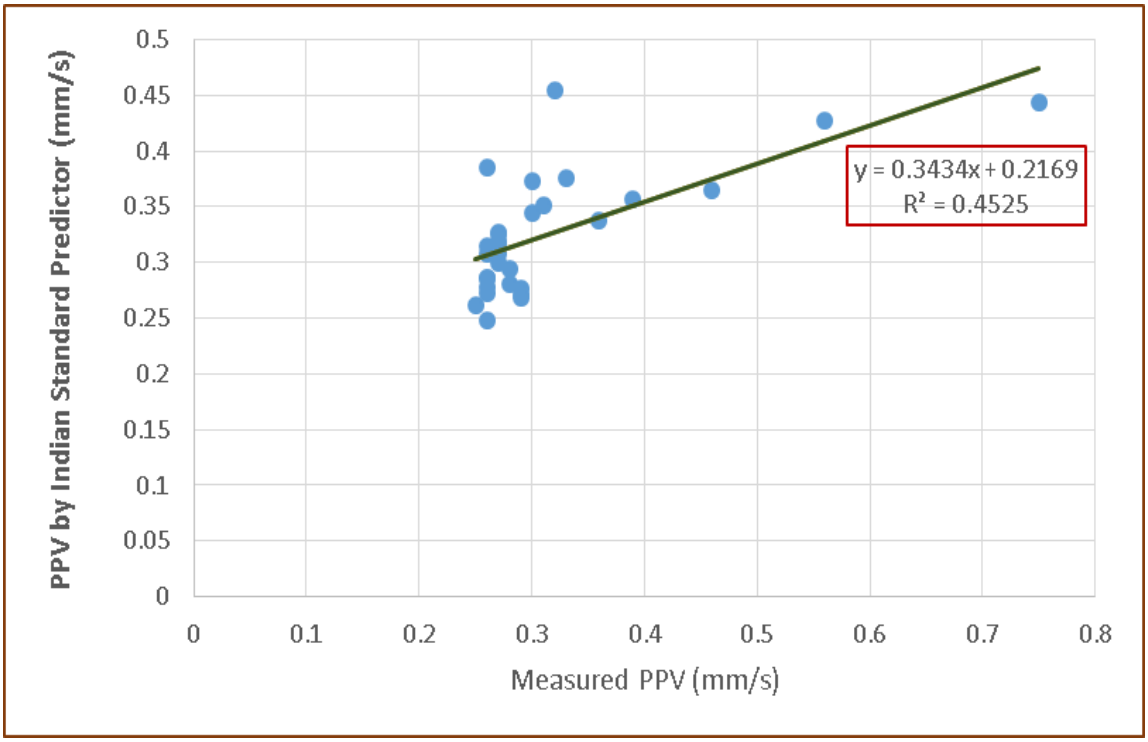

Figure 3.20. Measured and predicted PPV by Indian Standard Institute

Figures 3.17, 3.18, 3.19 and 3.20 above try establishing the relationship between measured and predicted PPV using empirical predictors. The graphs however have relatively low R^2 values signifying a weak relationship between the measured and predicted PPVs. The poor relationship is due to the inability of the empirical equations used to account for the inherent complexities present in the input parameters, hence the need for the ANN model.

3.6. EMPIRICAL PREDICTOR FOR AIRBLAST (AOp)

The cube-root scaled distance factor (SD) is generally used to predict AOp, in the absence of monitoring. The blasts are scaled to equivalent distances using the maximum charge per delay and the distance from blast to monitoring the point. The site-specific constants (K and B) are generated by plotting the log transformed air overpressures against the log transformed scaled distances. To evaluate performance of the empirical predictors, the same datasets used for testing and validating the ANN and regression models were applied. Figure 3.21 shows the cube-root scaled distance and air overpressure on log–log scale. The site-specific constants K=139.86 and B=-0.0559 are generated from Figure 3.21.

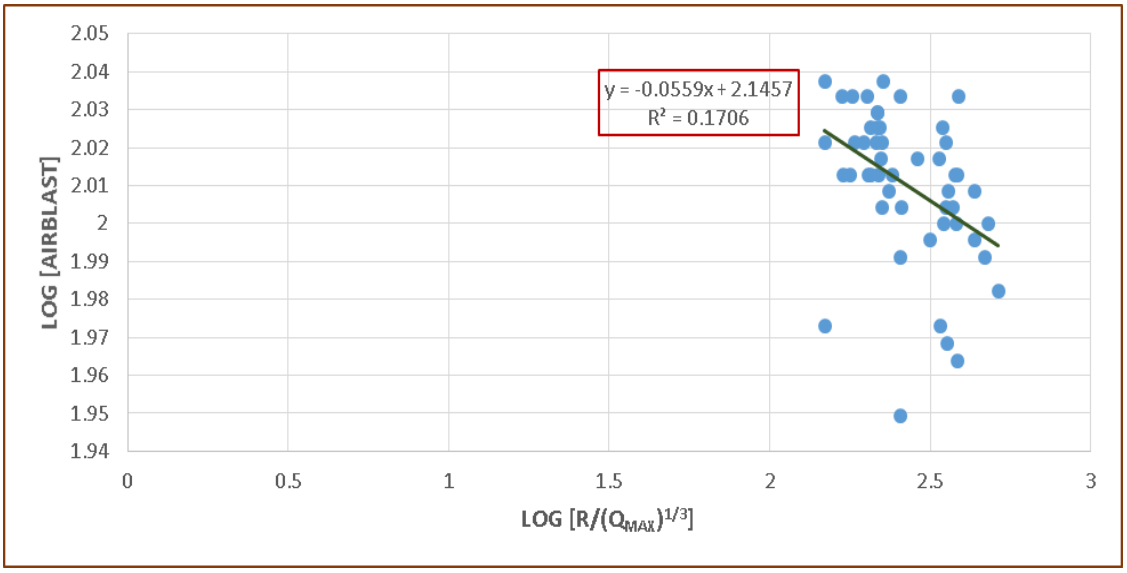

Figure 3.21. Airblast and scaled distance on log–log scale

There is a poor correlation between the airblast and the scaled distance as revealed by Figure 3.21 above.

The cube-root scaled distance empirical equation has been employed for the prediction of 30 data sets. Figure 3.22 below, illustrates the relationship between measured and predicted airblast using the cube-root scaled distance empirical predictor equation.

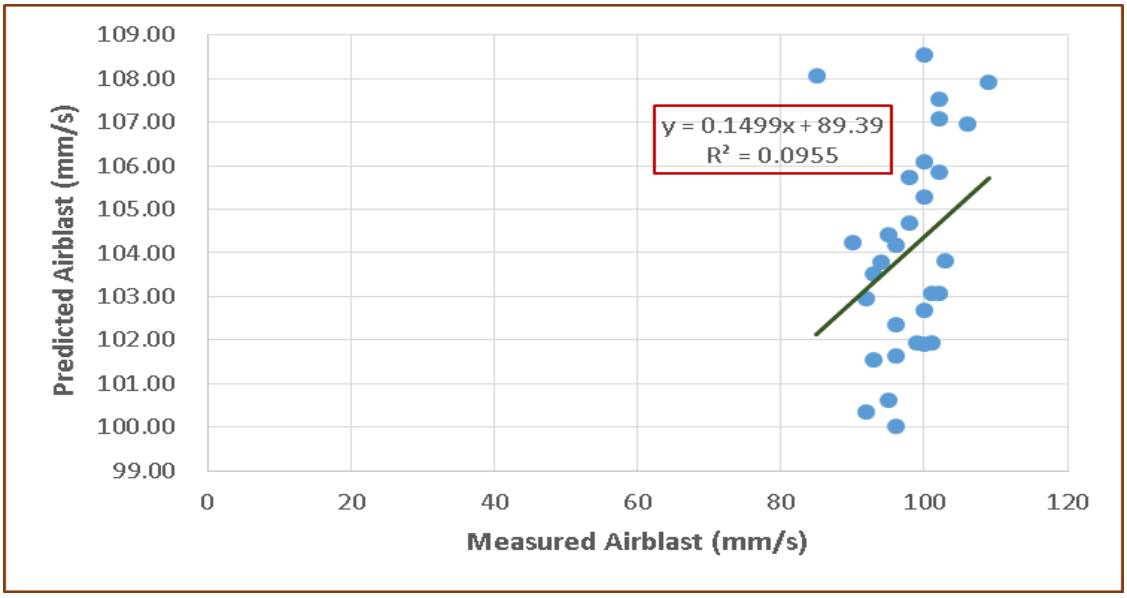

Figure 3.22. Measured and predicted Airblast

Airblast predictions by the cube-root empirical equation are not convincing with low R^2 of 0.0955 shown in Figure 3.22. This is due to the following (i) The cube-root empirical equation assumes just two input parameters (i.e. Maximum charge per delay and the distance from blast location to the monitoring point) and (ii) The cube-root empirical equation is not able to address the internal complexities present in the inputs. The ANN tool is therefore necessary to address the above flaws.

3.7. SENSITIVIY ANALYSIS

Sensitivity analysis was conducted on all the input parameters to ascertain the relative influence of each input parameter on rock fragmentation, ground vibration (PPV) and airblast (air over pressures). The sensitivity analysis was executed separately for the (i) rock fragmentation, (ii) ground vibration (PPV) and (iii) airblast (AOp). The cosine amplitude method (CAM) (Yang and Zang, 1997) was used to determine the strength of the connections between the input parameters and the output parameters under consideration. To apply this method, all the data pairs were expressed in common X-space. The data pairs were used to construct a data array X defined as:

$$X=\{x_1, x_2, x_3,\ldots x_i,\ldots x_n\} \tag{3.6}$$

Each of the elements, x_i, in the data array X is a vector of lengths, that is:

$$x_i=\{x_{i1},x_{i2},x_{i3},\ldots,x_{im}\} \tag{3.7}$$

Each of the data set can be thought of as a point in m-dimensional space, where each point requires m-coordinates for a full description. Thus, all points in the space have a relation with results pair wise. The strength of the relation (r_{ij}) between the dataset X_i and X_j is represented by the following equation:

$$r_{ij} = \frac{\sum_{k=1}^{m} x_{ik}x_{jk}}{\sqrt{\sum_{k=1}^{m} X_{ik}^2 \sum_{k=1}^{m} x_{jk}^2}} \tag{3.8}$$

The results of the sensitivity analyses for Peak particle velocity (PPV) is presented in Figure 3.23.

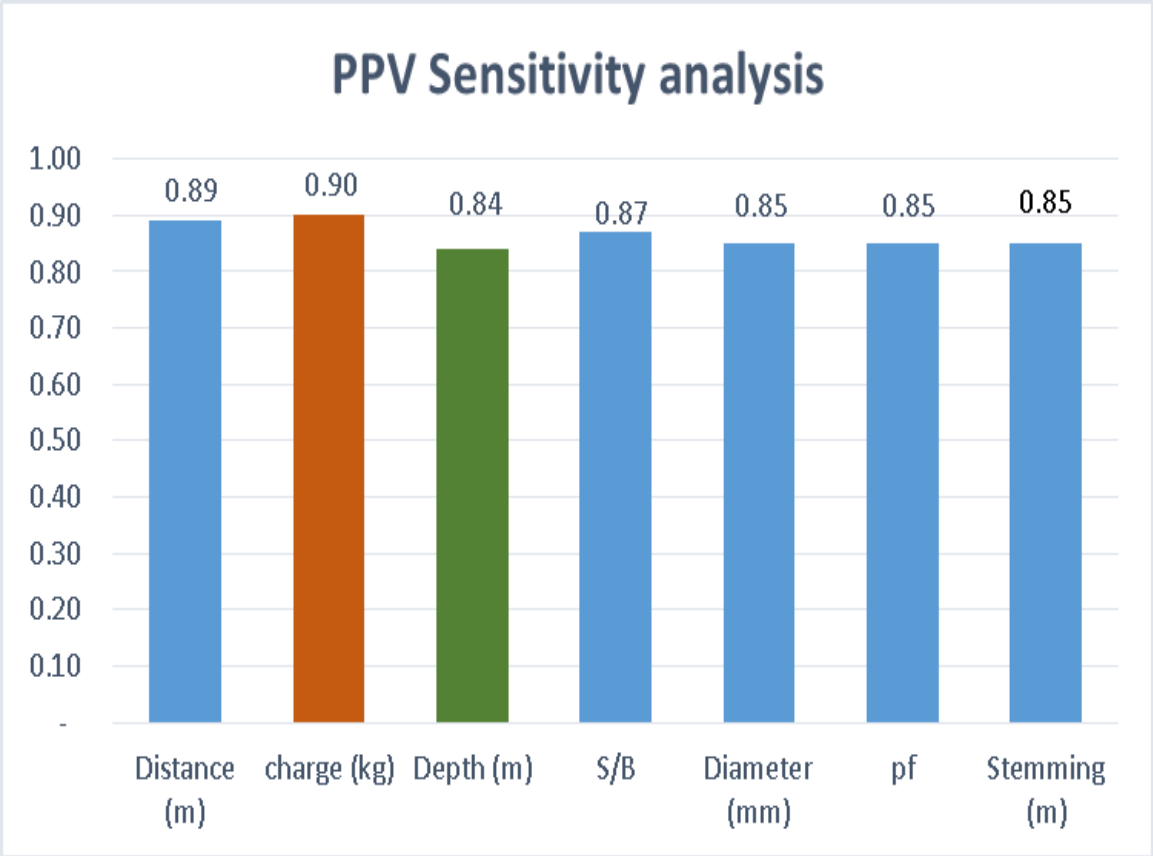

Figure 3.23. Sensitivity analysis of input parameters

From Figure 3.23 above, distance from blast face to monitoring point and the charge per delay are the most effective input parameters on the PPV, whereas, depth of hole is the least effective parameter. Practically, the impact of PPV on neighboring premises decreases with decreasing charge per hole and increasing distance from the center of action.

The results of the sensitivity analyses for airblast is illustrated in Figure 3.24.

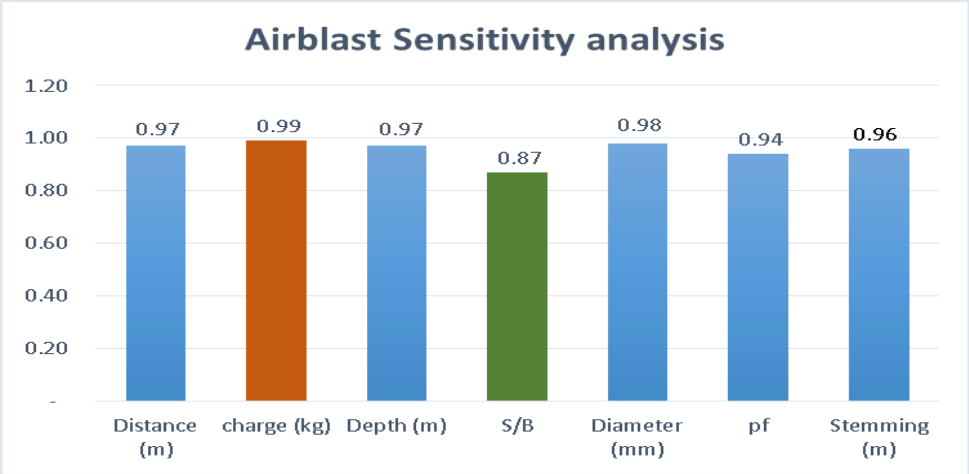

Figure 3.24. Sensitivity analysis of input parameters

While charge per delay influences airblast the most as presented in Figure 3.24 above, the ratio of spacing to burden has the least influence on airblast. The Diameter also bears an unusually high influence on the airblast.

The results of the sensitivity analyses for rock fragmentation is presented in Figure 3.25.

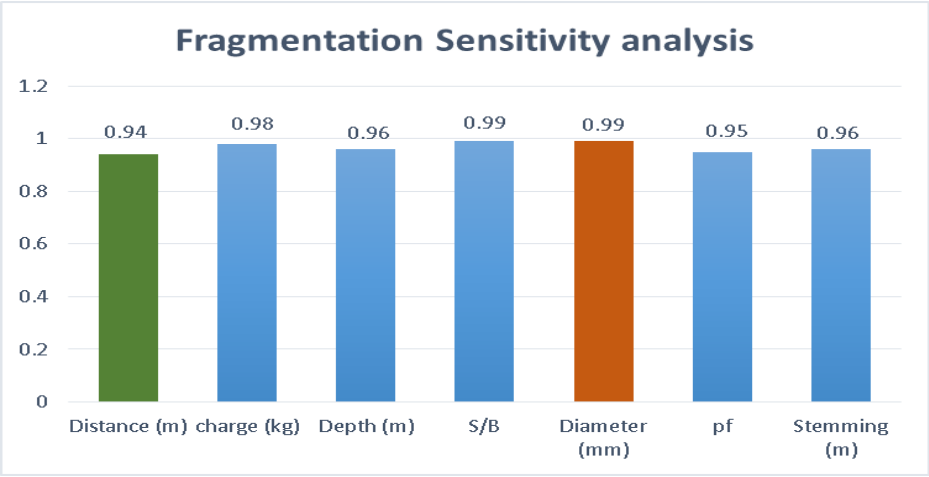

Figure 3.25. Sensitivity analysis of input parameter

As illustrated by Figure 3.25 above, the most influential factors on fragmentation are the diameter and spacing to burden ratio whiles the distance from the blast point to the monitoring area is the least sensitive factor.

3.8. SUMMARY

Dataset of inputs and their corresponding outputs are imported into the artificial neural network (ANN) system in MATLAB®. The ANN network is designed by defining the training function, the learning function, the transfer function and specifying the number of neurons in the hidden layer. The network is then trained, tested and validated. The performance of the ANN model can be improved by retraining or increasing the number of datasets. The network with the least RMSE is chosen as the optimum ANN model. This optimum ANN model is used to predict thirty (30) new dataset and the predicted outputs are compared with the real measured outputs to estimate the accuracy of the model. The results obtained from ANN model are much closer to reality, thus the ANN model is suitable for predicting new datasets in the field.

Multivariate regression analysis (MVRA) equations are also used to predict the same thirty (30) dataset and the predicted results are compared with the measured/actual outputs. Multivariate regression analysis (MVRA) predictors did not attain the desired level of accuracy. Ground vibrations (PPVs) and airblasts (AOps) are predicted using empirical equations based on the same dataset and the predicted outputs are compared with the measured outputs. Results demonstrate that the predicted outputs are not close to the actual outputs, thus not recommended for field predictions.

Linear curve fittings are used for comparing the predicted and actual outputs for the various predictive models in this section. This is due to the fact that most plots of actual and predicted datasets available in literature show a linear relationship. Moreover, linear curves make the analysis of uncertainty in dataset tractable and easy to interpret.

Finally, sensitivity analysis using the proposed ANN model is performed to ascertain the influence of each input parameter on rock fragmentation, ground vibration and airblast. Section 4 delves into the data analysis and discussions.

4. DATA ANALYSIS AND DISCUSSION

4.1. ANN AND MVRA ANALYSIS

Multivariate Regression Analysis (MVRA) tool used to predict PPV, airblast and fragmentation were mostly poor as demonstrated by Figures 3.10, 3.11 and 3.12 with the strongest relationship occurring for comparison between the predicted and measured fragmentation in Figure 3.11. RMSE and R^2 were used for comparing the artificial neural network (ANN) and the MVRA models. The indexes were calculated for the different output parameters belonging to the ANN and the MVRA models as shown in Table 4.1 below.

Table 4.1. Computed RMSE and R^2 for comparing ANN and MVRA models

Model	**Parameter**	**RMSE**	**R^2**
ANN	Ground vibration	0.018	0.970
	Airblast	0.290	0.996
	Rock fragmentation	0.316	0.997
MVR	Ground vibration	0.185	0.058
	Airblast	14.476	0.157
	Rock fragmentation	5.968	0.799

As observed from Table 4.1 above, the ANN model is more accurate than the MVRA model since the root mean square error (RMSE) for the different parameters in the ANN model are relatively smaller compared to those of the MVRA model for the same parameters. In addition, the coefficient of determination (R^2) for the parameters in

the ANN model is closer to unity compared to those of the MVRA. Hence, ANN model predicts outputs with suitable accuracy compared to MVRA model. Fragmentation prediction by the ANN model as seen in Table 4.1 is the best with R^2 of 0.997. MVR model also predicted rock fragmentation better than it did for airblast and ground vibration.

4.2. ARTIFICIAL NEURAL NETWORK AND EMPIRICAL PREDICTORS

Empirical equations were used to predict peak particle velocity (PPV) and air overpressure (AOp). R^2 was used for comparing artificial neural network (ANN) and empirical models. The R^2 index was calculated for the different output parameters belonging to ANN and empirical models as shown in Tables 4.2 and 4.3 below.

Table 4.2. R^2 for comparing predicted PPV using ANN and empirical models

Predictors	**R^2**
ANN	0.970
USBM	0.320
AMBRASEY-HENDRON	0.257
LANGEFORS–KIHLSTROM	0.452
INDIAN STANDARD PREDICTORS	0.452

Table 4.2 shows higher coefficient of determination (R^2) for the ANN predictor compared to the other empirical predictors. This is an indication that PPV is best-predicted using ANN predictors than employing the other empirical techniques.

Table 4.3. R^2 for comparing AOP using ANN and empirical model

Predictors	**R^2**
ANN	0.996
Cube-root scaled distance	0.096

Moreover, the ANN model in Table 4.3 above has a relatively high R^2 of 0.996. Thus, the ANN model is a better predictive model compared to the cube-root scaled distance empirical predictor.

4.3. BLAST OPTIMIZATION USING ARTIFICIAL NEURAL NETWORK

In order to improve the efficiency and quality of the blasting operations, the optimum ANN model developed was used to optimize ten (10) experimental blasts carried out at the mine and the results compared to ten (10) non-optimized blasts. Table 4.4 represents blast outputs and equipment statistics without ANN application.

Table 4.4. Blast outputs and equipment stats without ANN application

Airblast(Db)	PPV(mm/s)	Fragmentation (%)	Crusher Prdtivity (tonnes/day)	Ex. Prdtivity (bcm/hr)	Crusher Availabilities (%)	Exc. Availabilities (%)
118	0.95	75	15,200	256	77	75
117	0.76	68	13,788	355	75	80
116	1.65	76	19,556	312	81	78
122	1.46	75	16,359	298	76	77
119	1.33	78	21,456	306	80	79
121	1.33	75	17,894	311	77	77
122	1.02	70	15,263	388	76	81
119	0.81	78	20,015	287	80	77
116	0.71	65	13,329	355	69	81
119	1.27	70	14,896	222	75	74

Blast outputs and equipment statistics in Table 4.4 did not meet company requirements. The PPVs and AOps recorded were above the company set limits of 0.7mm/s and 115dB respectively. Crusher productivities were below the company's target of 23,000tonnes/day. Most rock fragments were outside the desired range with D80 around 0.7m following Split-Desktop analysis. Excavator productivities were poor compared to the company's target of 464bcm/hr. Excavator and crusher availabilities were lower than the company's target of 85% for both equipment.

Prior to blasting, the ANN model was used to simulate the input blast parameters until desired rock fragmentation, airblast and ground vibration were attained. This was done for ten (10) different blasts and the results illustrated in Figure 4.5. Table 4.5 shows blast outputs and equipment statistics following ANN analysis.

Table 4.5. Blast outputs and equipment stats following ANN analysis

Airblast(Db)	PPV(mm/s)	Fragmentation (%)	Crusher Prdtivity (tonnes/day)	Ex. Prdtivity (bcm/hr)	Crusher Availabilities (%)	Exc. Availabilities (%)
105	0.32	83	24,156	480	86	85
84	0.44	83	23,896	476	85	87
109	0.54	82	25,489	520	85	86
98	0.51	85	25,444	493	87	87
100	0.23	82	24,363	486	86	87
99	0.57	84	23,879	497	87	88
104	0.44	84	23,589	500	85	86
101	0.64	81	24,015	470	88	86
87	0.23	83	25,326	488	85	87
101	0.67	82	23,698	469	86	85

Blast outputs and equipment statistics presented in Table 4.5 is an indication of immense improvement following simulation on the input blast parameters using the optimum ANN model prior to blasting. The PPVs and AOps were within the confines of the company limits. Rock fragments were within desired range with D80 reduced from 0.7m to 0.45m. Improvements were made in the equipment productivities and availabilities as well. The crusher availabilities and productivities were improved by 11% and 31% respectively. There was also a 10% and 37% gain in the excavator availabilities and productivities respectively as illustrated by Table 4.6. Comparison of equipment statistics before and after the ANN model application is presented in Table 4.6.

Table 4.6. Comparison of equipment stats before and after ANN application

Equipment Statistics		Before	After	Percentage Increase (%)
Crusher	Availability(%)	77	86	11
	Productivity(bcm/hr)	16,776	24,386	31
Excavator	Availability(%)	78	86	10
	Productivity(bcm/hr)	309	488	37

Sample improved fragmentation and uniform pit floor after implementing optimum ANN model are displayed by Figures 4.1 and 4.2 respectively.

Figure 4.1. Improved fragmentation

Figure 4.2. Uniform pit floor

Figure 4.1 shows improved rock fragmentation following ANN application. Improved fragmentation reflected in the uniformity of the pit floor as indicated by Figure 4.2.

4.4. SENSITIVITY ANALYSIS

Sensitivity analysis was conducted on all the input parameters to determine the relative influence of each input parameter on rock fragmentation, ground vibration (PPV) and airblast (AOps). From Figure 3.21, distance from the blast face to the monitoring point and the charge per delay are the most effective input parameters for the PPV, whereas the depth of hole is the least effective parameter. Practically, the impact of PPV on neighboring premises decreases with decreasing the charge per hole and increasing the distance from the center of action. While charge per delay influences airblast the most as presented by Figure 3.22, the ratio of spacing to burden has the least influence on airblast. The Diameter also bears an unusually high influence on the airblast. As illustrated by Figure 3.23, the most influential factors on fragmentation are diameter and spacing to burden ratio whiles the distance from the blast point to the monitoring area is the least influencing factor.

4.5. SUMMARY

Artificial neural network (ANN) model proved to be more effective compared to the multivariate regression analysis (MVRA) and empirical equations. The optimum ANN model improved the efficiency of the blast operation by reducing the ground vibration and airblast values below company threshold limits of 0.7mm/s and 115dB respectively. Most of the rock fragments were within desired range with D80 reduced from 0.7m to 0.45m. The distance from blast face to monitoring point and the maximum charge per hole proved the most effective parameters whiles depth the least effective parameter on PPV following sensitivity analysis. The maximum charge per delay was the most sensitive parameter on AOp whiles the spacing to burden ratio was the least sensitive parameter. The most influential input parameters on fragmentation were diameter and the ratio of spacing to burden. Distance had the least influence on

fragmentation. Conclusions and recommendations for future work are presented in section 5.

5. CONCLUSIONS AND RECOMMENDATIONS FOR FUTURE WORKS

5.1. CONCLUSIONS

The study was geared towards improving fragmentation, minimizing blast impacts and protecting communities within the immediate premises of the blasting operations. An optimum ANN model was developed and used at Perseus Mines. The results of ANN predictions were then compared to empirical techniques and MVRA predictors. The ANN model generated was again used to optimize a set of blasts and the results compared to a set of non-optimized blasts and the equipment availabilities and productivities were captured. The ANN model improved fragmentation and minimized blast impacts. Results obtained from the study and their validations are summarized below:

1. Optimum artificial neural network (ANN) model is generated with:
   (i) Architecture 7-13-3.
   (ii) RMSE (0.307) and R^2 (0. 999).
2. Optimum ANN model improved the efficiency of the blast operation by reducing ground vibration and airblast values below company limits of 0.7mm/s and 115dB respectively. Rock fragments were within the desired range with D80 reduced from 0.7m to 0.45m. There was a 31% and 37% improvement in crusher and excavator productivities respectively. Crusher availability went up by 11% while excavator availability increased by 10% following the application of the ANN model.
3. Artificial neural network (ANN) model proved to be more effective compared to empirical equations and multivariate regression (MVR) matching their respective RMSE and R^2.
4. The distance from blast face to monitoring point and the maximum charge per delay proved the most effective parameters whiles depth the least effective parameter on PPV following sensitivity analysis.
5. The maximum charge per delay was the most sensitive parameter on AOp whiles the spacing to burden ratio was the least sensitive parameter on AOp.

6. The most influential input parameters on fragmentation were diameter and the ratio of spacing to burden. Distance had the least influence on fragmentation.
7. In addition to using the optimum ANN model, it is recommended that best blasting practices including proper planning, close supervision, correct delay times and initiation pattern selection, properly selected stemming material and accurate drilling among others should be considered for best results.

5.2. RECOMMENDATIONS FOR FUTURE WORK

This research has produced significant evidence that ANN models are best for predicting fragmentation and blast impacts. Further studies are required to enhance work carried out in this study as discussed below:

1. The input parameters could be expanded to include mechanical and geotechnical rock parameters such as rock strength, RQD, rock hardness, number of joints etc. to provide the ANN model a wider platform to operate.
2. Other ill effects resulting from poor blasts such as fly rocks and back breakes among others could be considered in the outputs since their impacts on production and immediate communities are significant.
3. Optimum ANN performance could be enhanced by combining ANN model with other algorithms such as particle swarm optimization algorithm, imperialist competitive algorithm (ICA) etc.

APPENDIX A

ARTIFICIAL NEURAL NETWORK (ANN) ARCHITECTURE

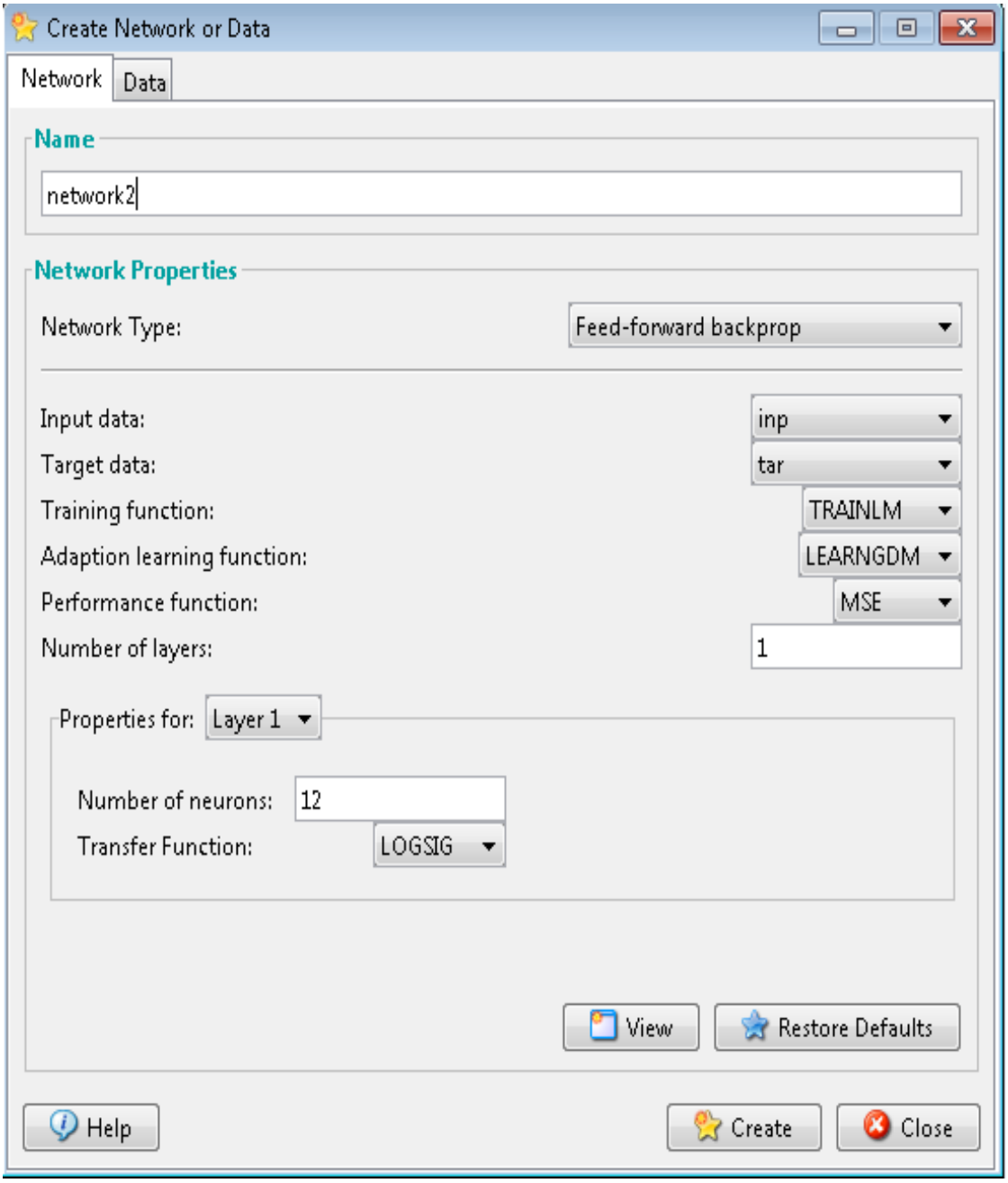

Typical ANN network creation interface

The network type, the training function, the learning function, and transfer function among others are properly defined here before training begins.

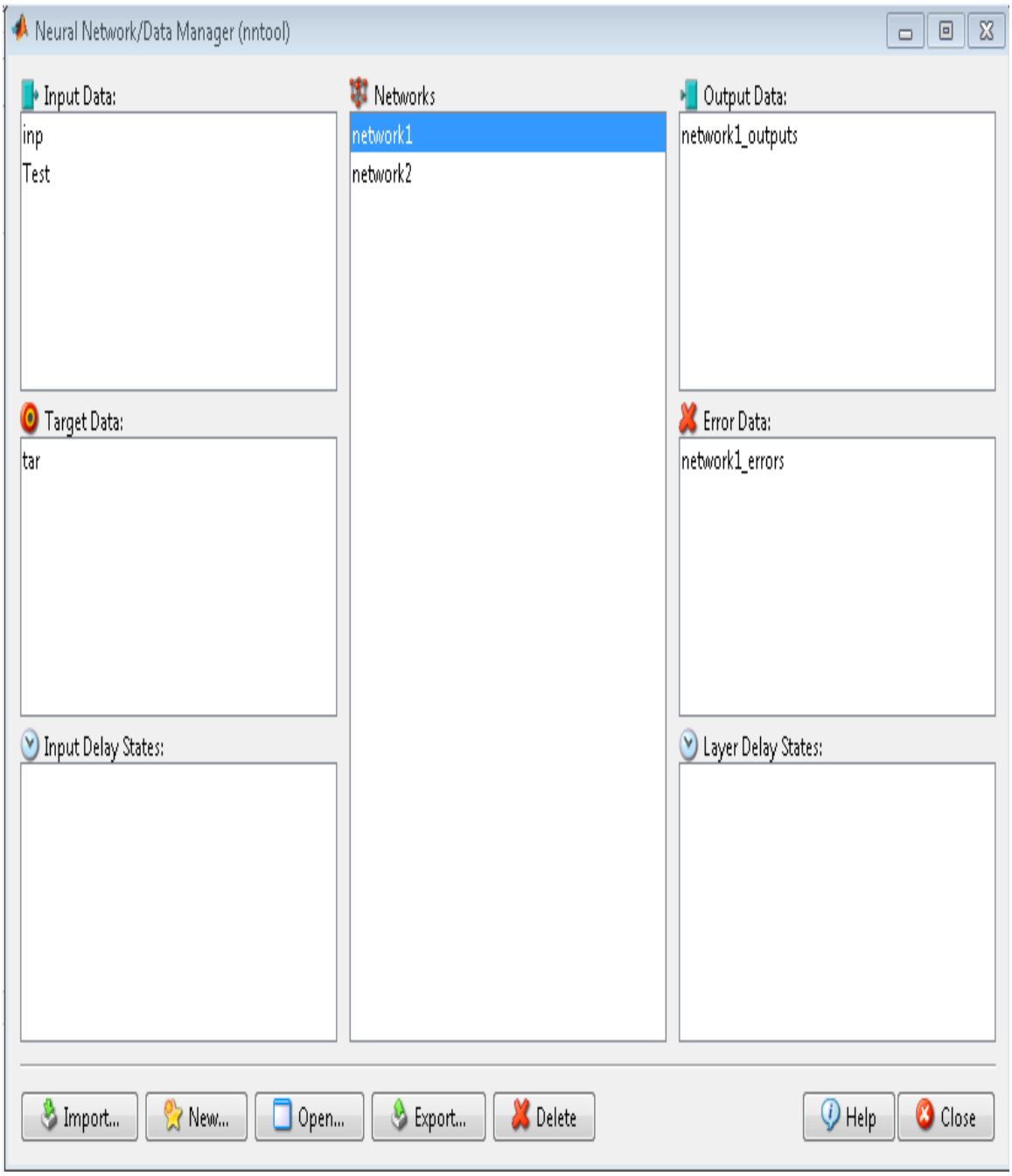

Typical ANN network data manager for nntool

The different networks created are available here for selection and further processing. All data imported into system are displayed here.

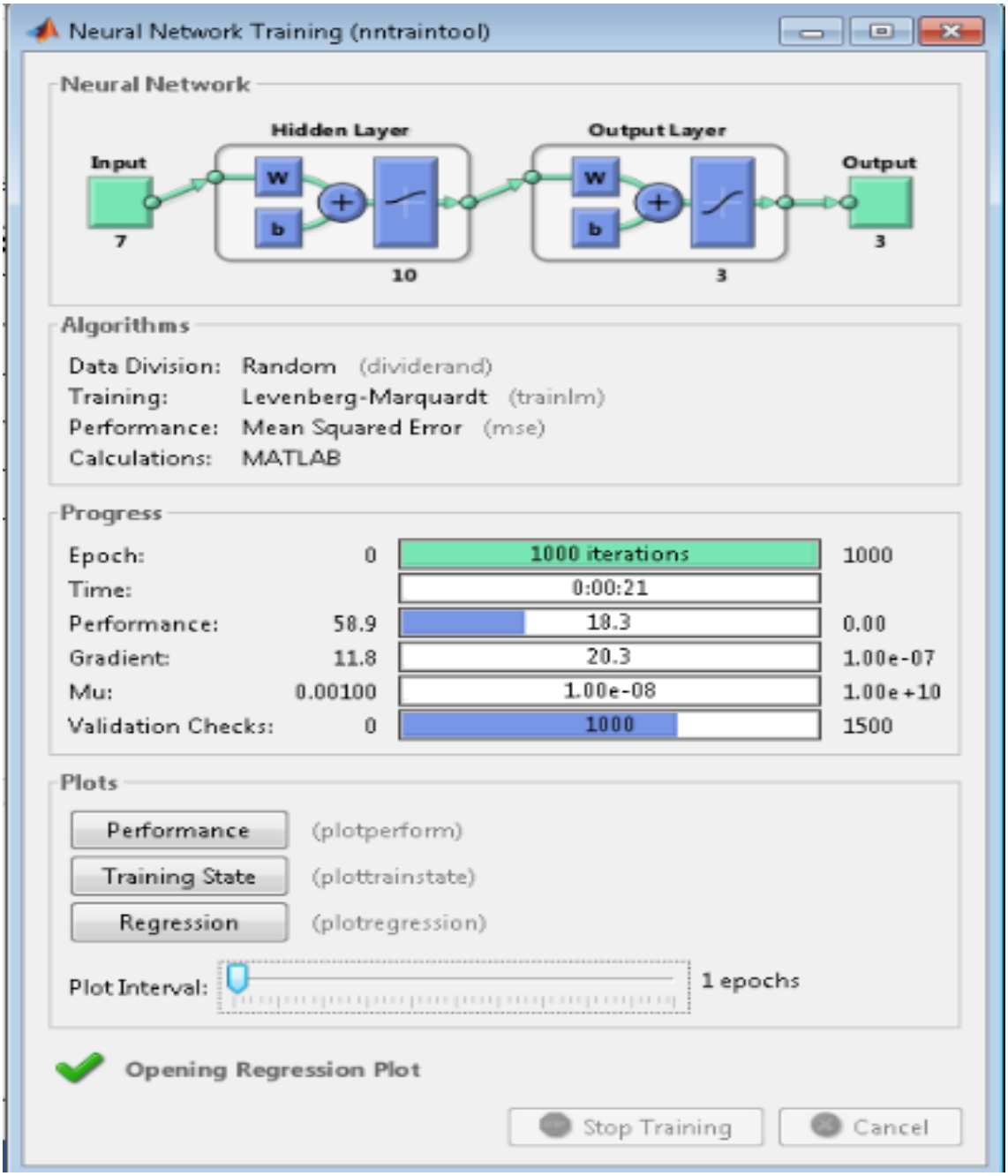

Neural network training tool

Regression plot can be displayed for correlation between output data and target data. Retraining can be conducted to improve performance.

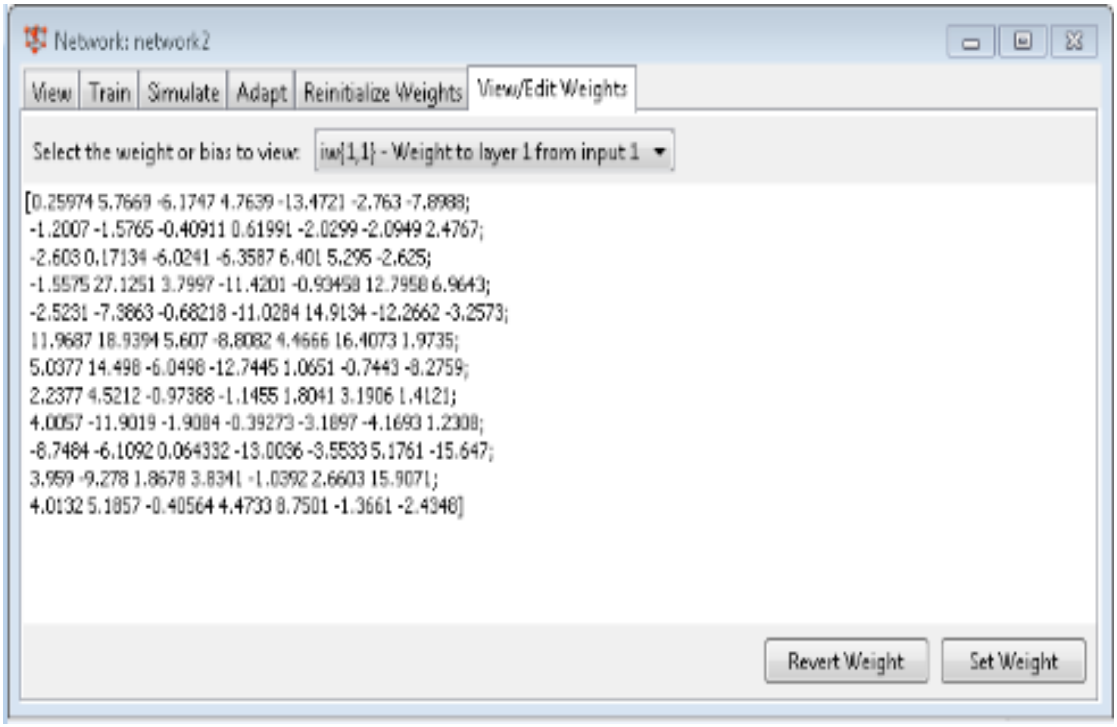

Weight adjustment tab

Weights can be modified to improve performance.

APPENDIX B
TRANSFER FUNCTIONS TESTED

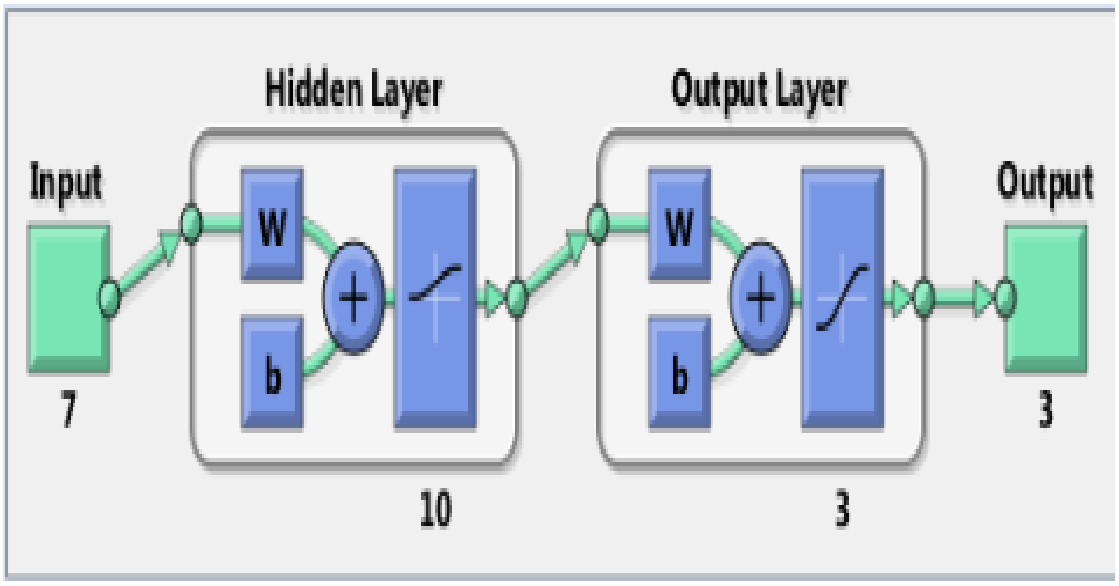

Custom Logsin view (Ten neurons)

The transfer function used above is the Logsin with architecture 7-12-3

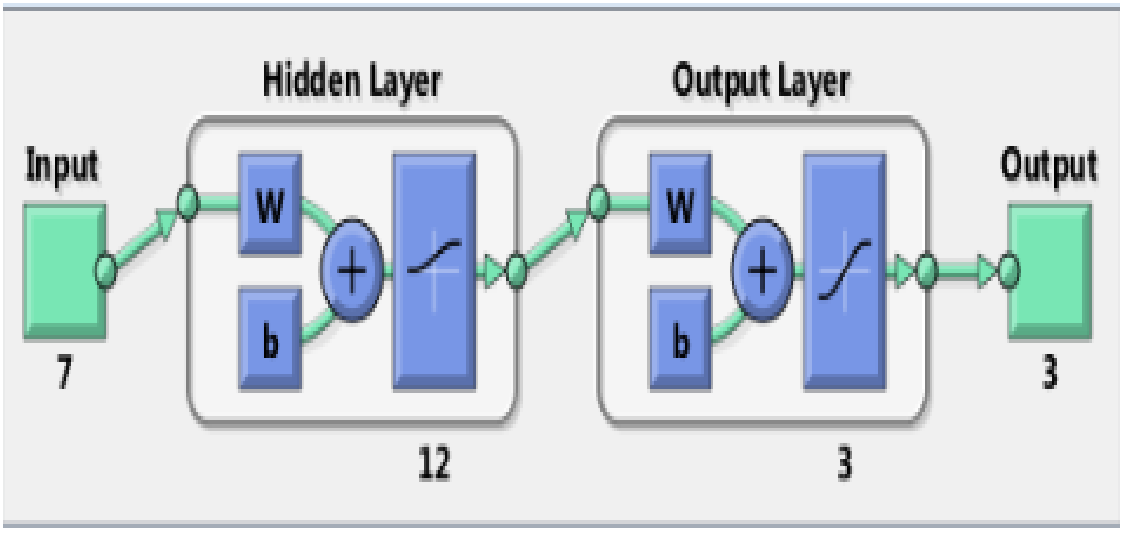

Custom Logsin view (twelve neurons)

The transfer function used above is the Logsin with architecture 7-12-3

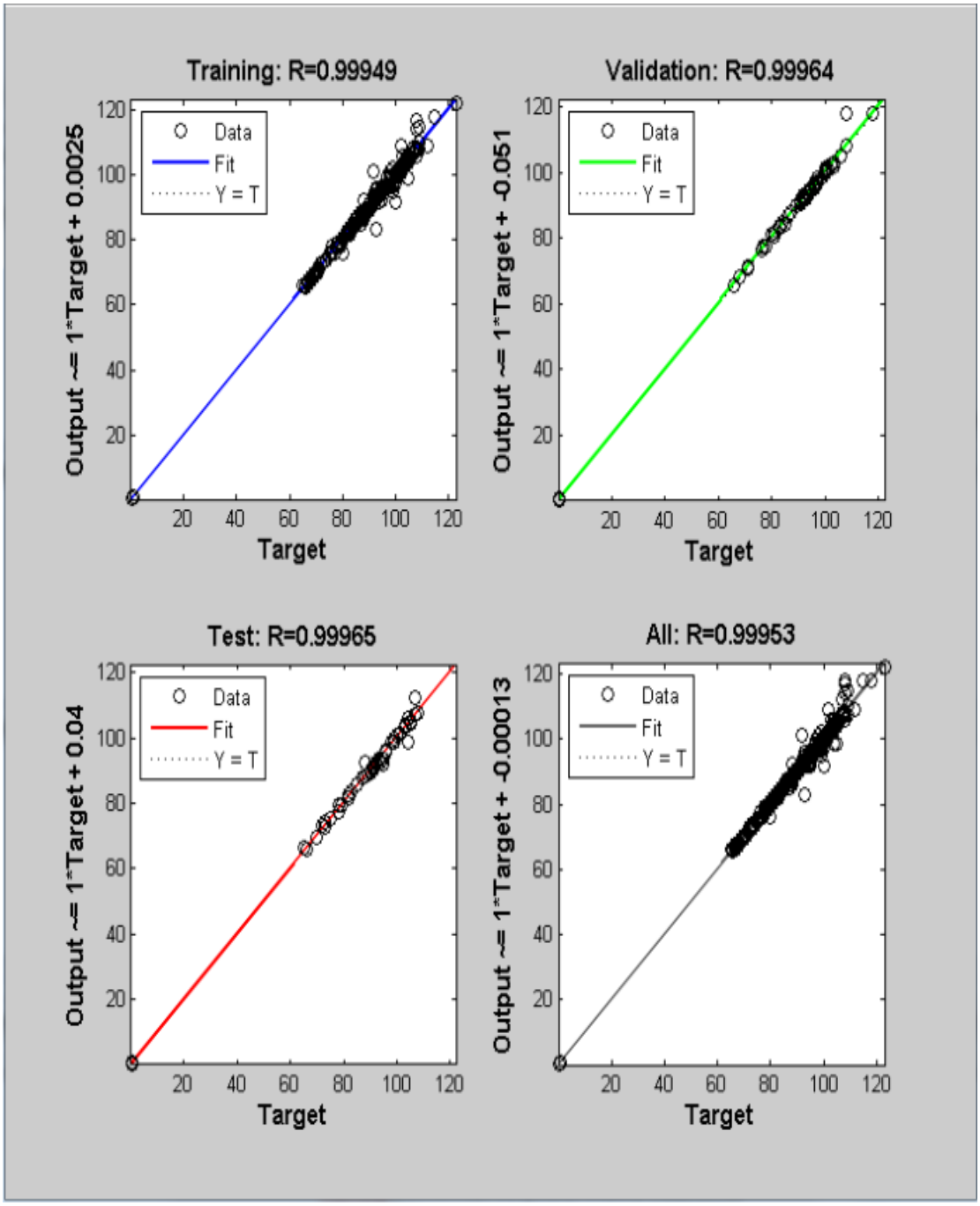

Neural network training regression plot for Logsin (Ten neurons)

Correlations between output and target data for training data, validation data, testing and the entire data set are displayed in the plot above.

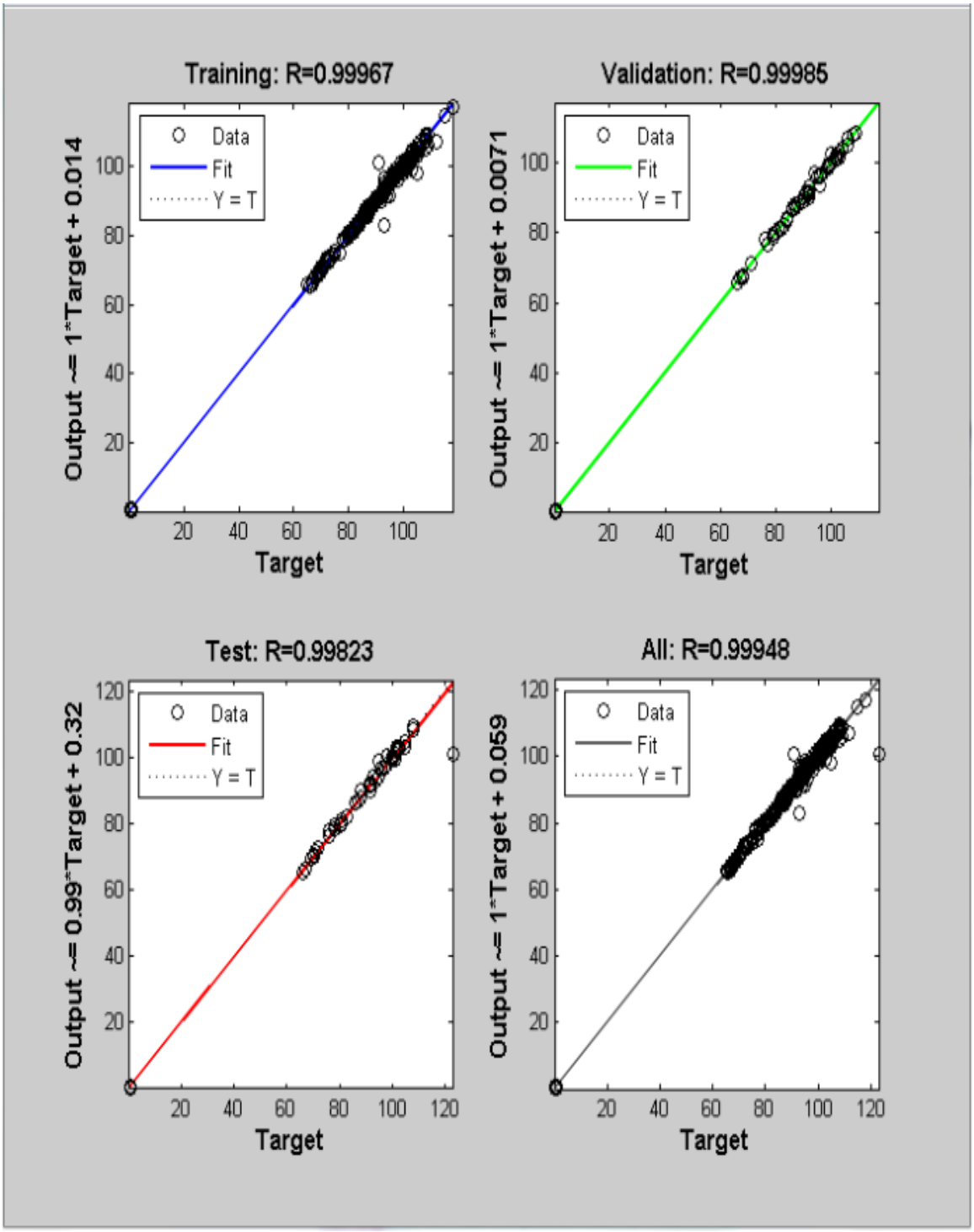

Neural network training regression plot for Logsin (Twelve neurons)

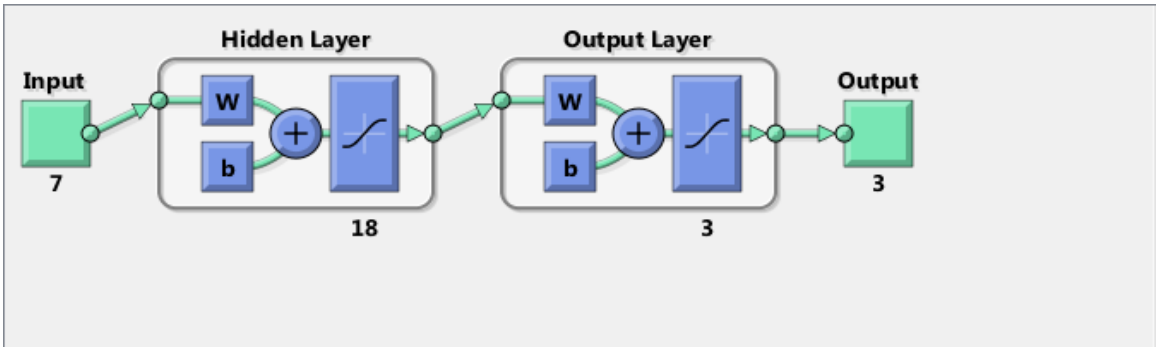

Custom Tansig view (eighteen neurons)

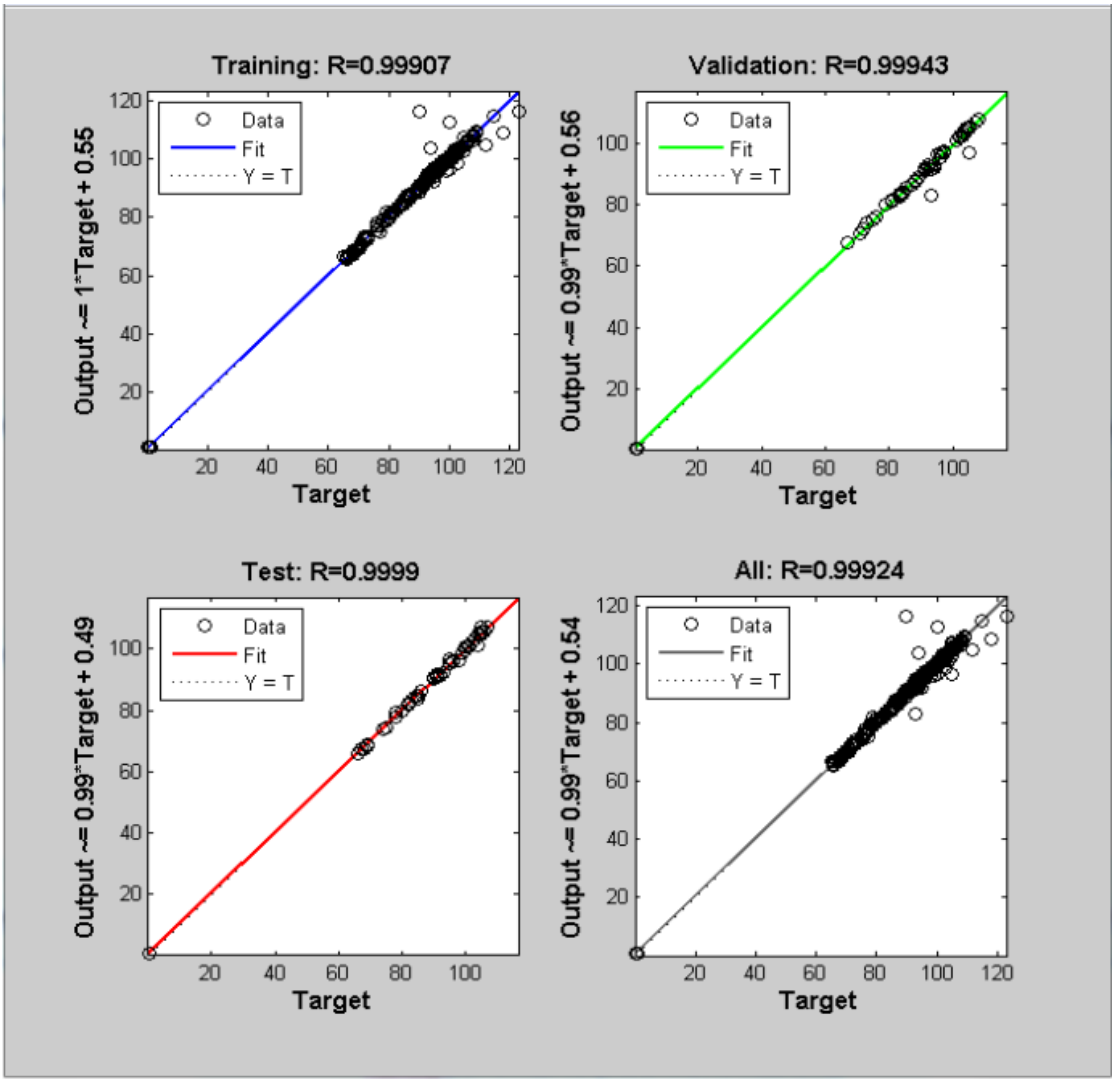

Neural network training regression plot for Tansig (eighteen neurons)

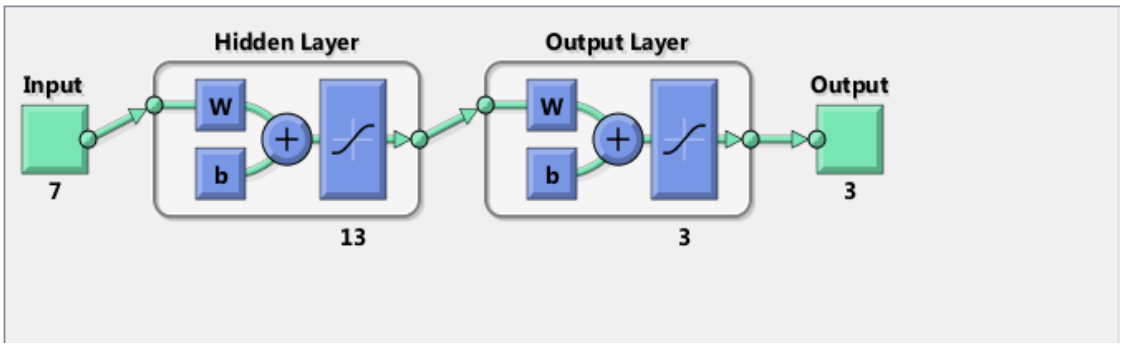

Custom Tansig view (Thirteen neurons)

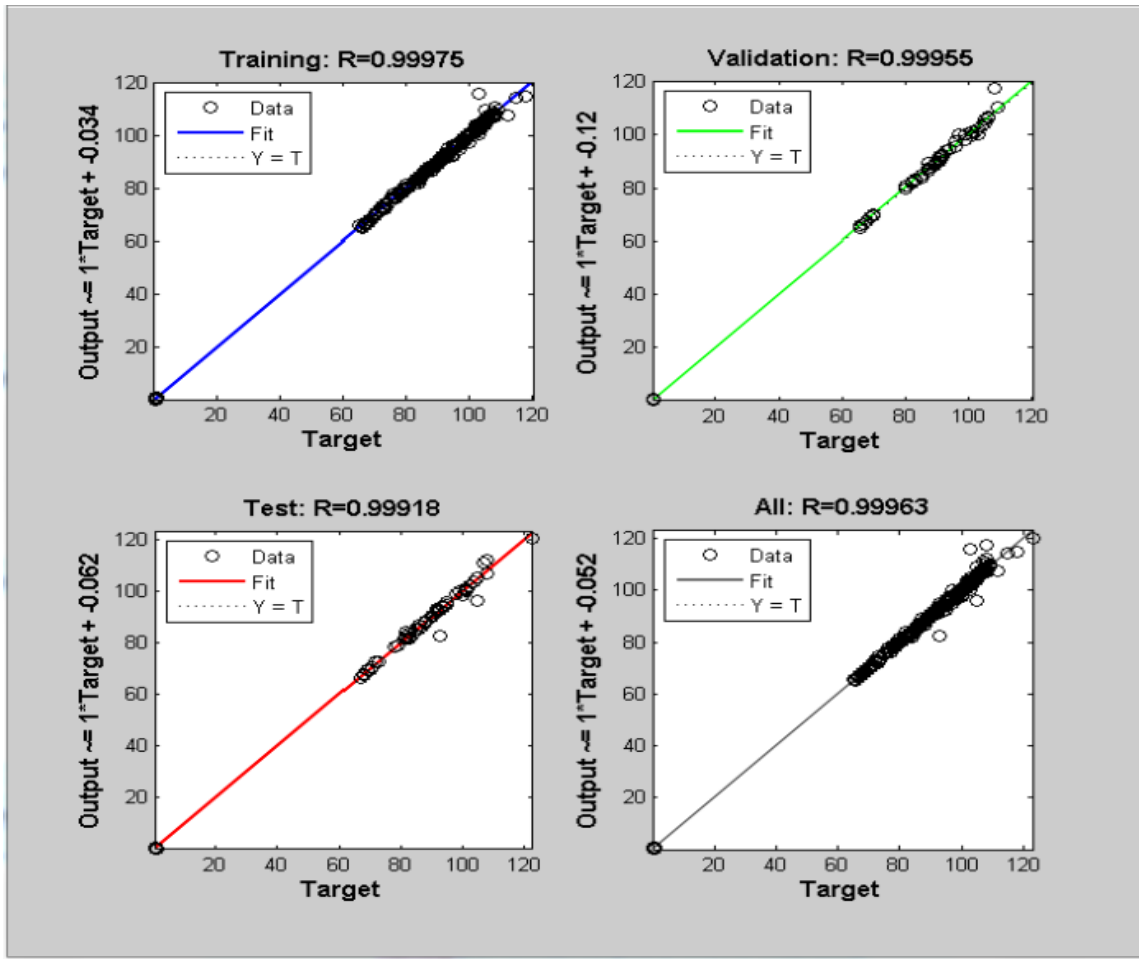

Neural network training regression plot for Tansig (Thirteen neurons)

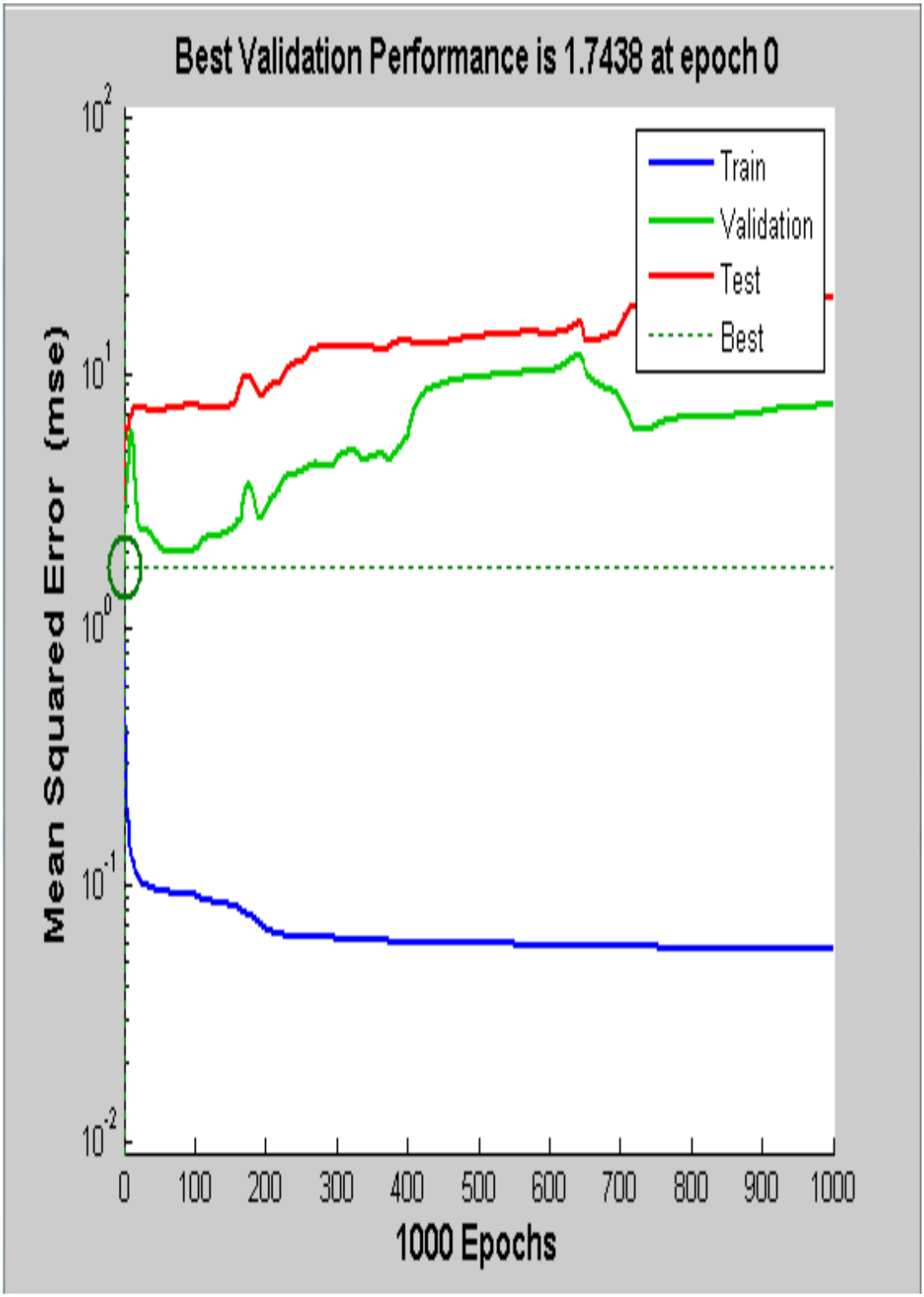

Tansig performance plot (Thirteen neurons)

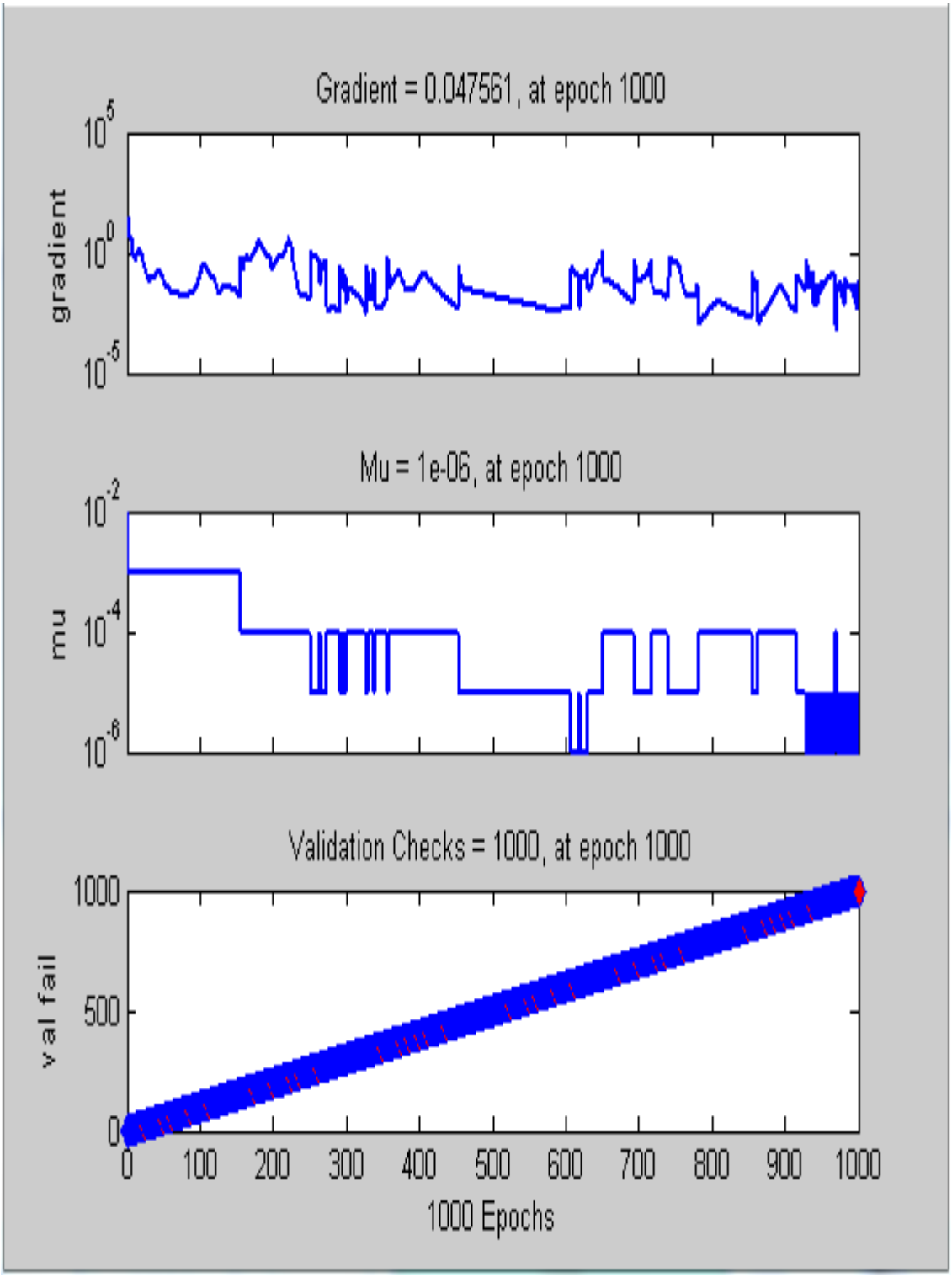

Tansig training state plot (Thirteen neurons)

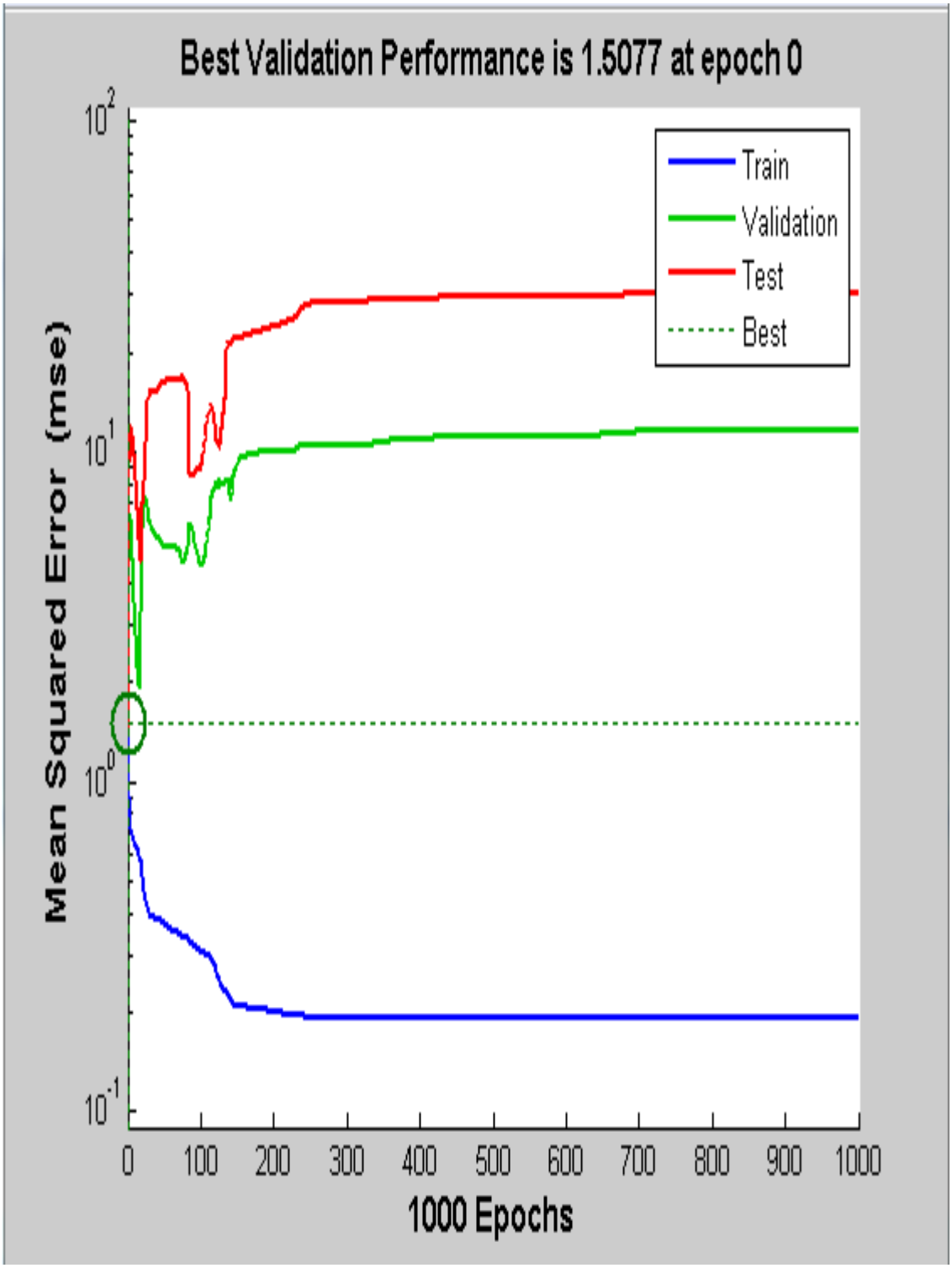

Tansig performance plot (Ten neurons)

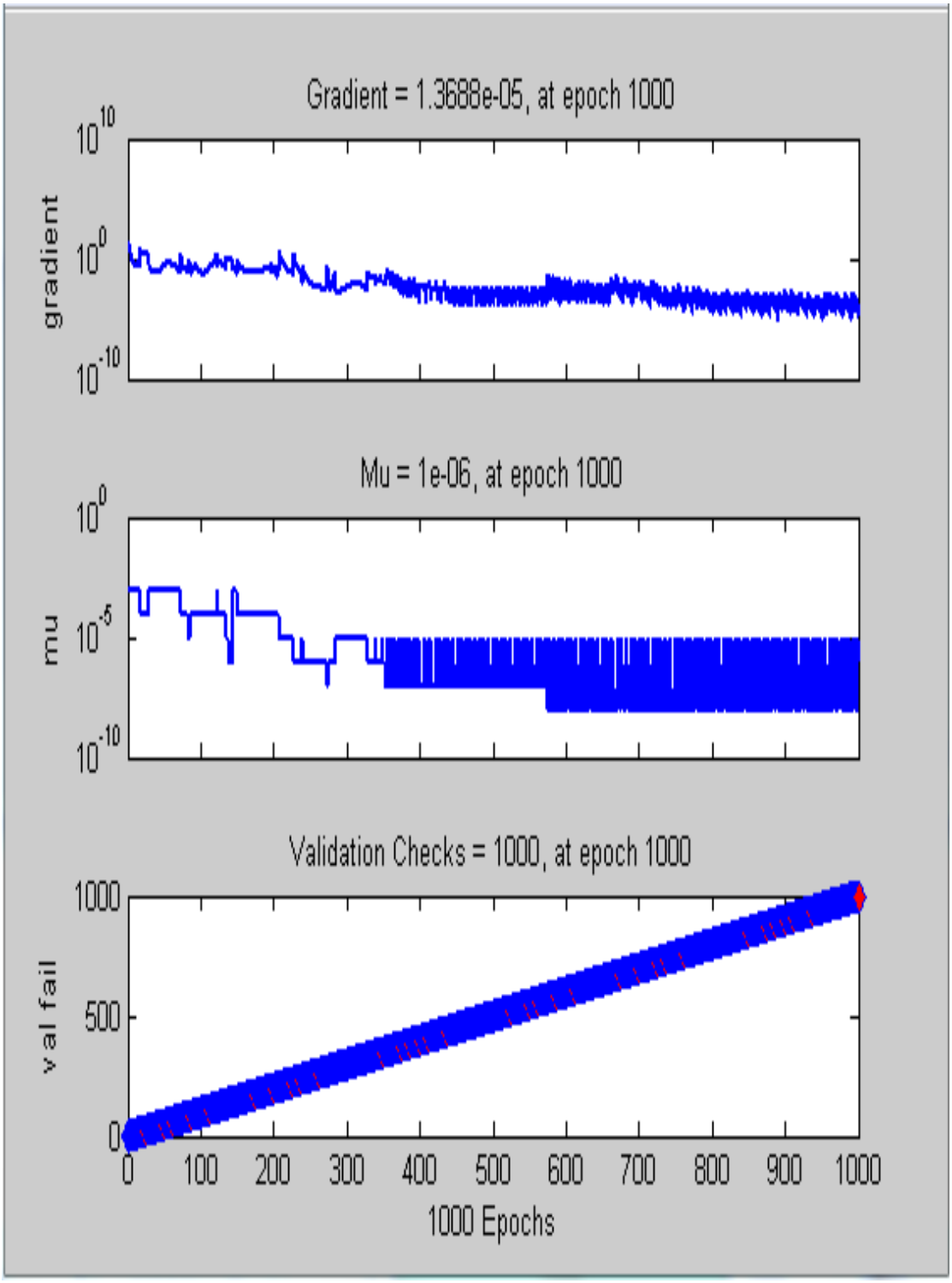

Tansig training state plot (Ten neurons)

REFERENCES

[1] Enayatollahi, Iman; Aghajani Bazzazi, Abbas; Asadi, Ahamad, 2014. Comparison between Neural Networks and Multiple Regression Analysis to Predict Rock Fragmentation in Open-Pit Mines. Rock Mechanics and Rock Engineering, Volume 47, Issue 2, pp. 799 – 807.

[2] Khandelwal, Manoj and Singh, T.N., 2009. Prediction of blast-induced ground vibration using artificial neural network. International Journal of Rock Mechanics and Mining Sciences, Volume 46, Issue 7, pp. 1214 – 1222.

[3] M. Hajihassani; D. Jahed Armaghani; H. Sohaei; E. Tonnizam Mohamad; A. Marto., 2014. Prediction of airblast-overpressure induced by blasting using a hybrid artificial neural network and particle swarm optimization. Applied Acoustics, Volume 80, pp. 57 – 67.

[4] Monjezi, M; Bahrami, A; Yazdian Varjani, A., 2010. Simultaneous prediction of fragmentation and flyrock in blasting operation using artificial neural networks. International Journal of Rock Mechanics and Mining Sciences, Volume 47, Issue 3, pp. 476 – 480.

[5] Neaupane, Krishna Murari, and N. R. Adhikari, 2006. Prediction of tunneling-induced ground movement with the multi-layer perceptron. *Tunnelling and Underground Space Technology* 21.2, 151-159.

[6] Monjezi, M., Rizi, S. H., Majd, V. J., and Khandelwal, M., 2014. Artificial neural network as a tool for backbreak prediction. *Geotechnical and Geological Engineering*, *32*(1), 21-30.

[7] P.K. Simpson, 1990. Artificial Neural Systems. Foundation, Paradigms, Applications, and Implementations. Pergamon Press, New York, NY.

[8] Yang Y, Zang O., 1997. A hierarchical analysis for rock engineering using artificial neural networks. Rock Mech Rock Eng 30:207-222.

[9] Adel Greg, Toni Kojovic, and Darren Thornton, 2006. Mine-to-Mill Optimization of Aggregate Production. Virginia Polytechnic Institute & State University.

[10] Bahrami, A., Monjezi, M., Goshtasbi, K., & Ghazvinian, A., 2011. Prediction of rock fragmentation due to blasting using artificial neural network. *Engineering with Computers*, *27*(2), 177-181.

[11] Sayadi, A., Monjezi, M., Talebi, N., and Khandelwal, M., 2013. A comparative study on the application of various artificial neural networks to simultaneous prediction of rock fragmentation and backbreak. *Journal of Rock Mechanics and Geotechnical Engineering*, *5*(4), 318-324.

[12] Mackenzie AS, 1966. Cost of explosives-do you evaluate it properly. Mining Cong J 54:32–41.

[13] Kanchibotla S., 2001. Optimum blasting? Is it minimum cost per broken rock or maximum value per broken rock? Proceedings of Explo, Australasian institute of mining and metallurgy.

[14] Hustrulid W., 1999. Blasting principles for open pit mining, vol1. A.A. Balkema, Rotterdam.

[15] Atasoy, Y., Valery, W., & Skalski, A., 2001. Primary versus secondary crushing at St Ives (WMC) SAG mill circuit. In *SAG 2001* (Vol. 1, pp. 248-261). University of British Columbia.

[16] Michaux S, Djordjevic N., 2005. Influence of explosive energy on the strength of the rock fragments and SAG mill throughput. Miner Eng 18:439–448.

[17] Richards, A, 2010. Elliptical airblast overpressure model. Mining Technology, ISSN 1474-9009, Volume 119, pp. 205-211.

[18] Kuzu, C; Fisne, A; Ercelebi, S.G, 2009. Operational and geological parameters in the assessing blast induced airblast-overpressure in quarries. Applied Acoustics, ISSN 0003-682X, Volume 70, Issue 3, pp. 404 – 411.

[19] Monjezi, M., Amiri, H., Farrokhi, A., & Goshtasbi, K., 2010. Prediction of rock fragmentation due to blasting in Sarcheshmeh copper mine using artificial neural networks. *Geotechnical and Geological Engineering*, *28*(4), 423-430.

[20] Wu, Chengqing and Hao, Hong, 2007. Modeling of simultaneous ground shock and airblast pressure on nearby structures from surface explosions. International Journal of Impact Engineering, ISSN 0734-743X, Volume 31, Issue 6, pp. 699 – 717.

[21] Baker, W. E., Cox, P. A., Kulesz, J. J., Strehlow, R. A., & Westine, P. S., 2012. *Explosion hazards and evaluation* (Vol. 5). Elsevier.

[22] Technical Manual (TM-5-855-1), 1986. Fundamentals of protective design for conventional weapons. Headquarters, Department of the Army, Washington, DC.

[23] Bulson PS, 1997. Explosive loading of engineering structures. Macmillan Publishers New Zealand Ltd., E&FN SPON, an Imprint of Chapman & Hall.

[24] Mohanty B. Physics of explosions hazards, 1998. In: Beveridge A. editors, Forensic investigation of explosions. London; p. 22–32.

[25] Persson PA, Holmberg R, Lee J. Rock blasting and explosives engineering, 1994. In: editors, C.R.C. Press; pp. 375–86, 515.

[26] R.B. Hopler (Ed.), 1998. Blasters' handbook, International Society of Explosives Engineers.

[27] Siskind DE, Stachura VJ, Stagg MS, Koop JW, 1980. Structure response and damage produced by airblast from surface mining. United States Bureau of Mines Report of Investigation 8485.

[28] Dusenberry, Donald, 2010. Handbook for Blast Resistant Design of Buildings, pages 8-9.

[29] Tawadrous AS., 2006. Evaluation of artificial neural networks as a reliable tool in blast design. Int Soc Explos Eng, 1,1–12.

[30] Rezaei, M., Monjezi, M., Moghaddam, S. G., & Farzaneh, F., 2012. Burden prediction in blasting operation using rock geomechanical properties. *Arabian Journal of Geosciences*, *5*(5), 1031-1037.

[31] Sarkar, Kripamoy, Avyaktanand Tiwary, and T. N. Singh, 2010. Estimation of strength parameters of rock using artificial neural networks. *Bulletin of engineering geology and the environment*, 69.4, 599-606.

[32] Duvall WI, Johnson CF, Meyer AVC, 1963. Vibrations from instantaneous and millisecond delay quarry blasts. RI. 6151. US, Bureau of Mines, United States Department of Interior, Washington.

[33] Nicholls HR, Johnson CF, Duvall WI., 1971. Blasting vibrations and their effects on structures. Bulletin Washington, DC, Bureau of Mines, no. 656.

[34] Siskind DE, Crum SV, Otterness RE, Kopp JW., 1989. Comparative study of blasting vibrations from Indiana surface coal mines. RI 9226, USBM.

[35] Elseman I, Rasoul A., 2000. Measurement and analysis of the effect of ground vibration induced by blasting at the limestone quarries of the Egyptian cement company. Cairo University, Egypt.

[36] Monjezi, Masoud, Mahdi Hasanipanah, and Manoj Khandelwal, 2013. Evaluation and prediction of blast-induced ground vibration at Shur River Dam, Iran, by artificial neural network. *Neural Computing and Applications*, 22.7-8: 1637-1643.

[37] Hagan TN., 1973. Rock breakage by explosives. In: Proc Natl Symp on Rock Fragmentation, Adelaide, Australia, pp 1–17.

[38] Mostafa TM., 2009. Artificial neural network for prediction and control of blasting vibrations in Assiut (Egypt) limestone quarry. Int J Rock Mech Min Sci 46(2):426–431.

[39] McKenzie, C., 1990. Quarry Blast Monitoring Technical and Environmental Perspective, Quarry Management, pp. 23–29.

[40] Duvall, W.I., Fogleson, D.E., 1962. Review of criteria for estimating damage to residences from blasting vibrations. USBM, RI, vol. 5968, p. 19.

[41] Ghosh, A., Daemen, J.K., 1983. A simple new blast vibration predictor. In: Proc. 24th US Symp. Rock Mechanics, Texas, USA, pp. 151–161.

[42] N.R. Ambraseys, A.J. Hendron, 1968. Dynamic behaviour of rock masses: rock mechanics in engineering practices Wiley, London.

[43] W.J. Birch, R. Chaffer, 1983. Prediction of ground vibration from blasting on opencast sites. Trans. Inst. Mining Metall., Section A: Mining Ind., pp. A102–A107.

[44] Bureau of Indian Standard, 1973.Bureau of Indian Standard. Criteria for safety and design of structures subjected to underground blast. ISI Bulletin IS-6922.

[45] Khandelwal, Manoj, D. Lalit Kumar, and Mohan Yellishetty, 2011. Application of soft computing to predict blast-induced ground vibration. *Engineering with Computers*, pp. 117-125.

[46] U. Langefors, B. Kihlstrom, 1963. The modern technique of rock blasting. Wiley, New York.

[47] B. Davies, I.W. Farmer, P.B. Attewell, 1964.Ground vibrations from shallow sub-surface blasts. The Engineer, London, pp. 553–559.

[48] C.H. Dowding, 1985.Blast Vibration Monitoring and Control Prentice-Hall Inc., Englewood's Cliffs pp. 288–290.

[49] Khandelwal, Manoj, and T. N. Singh, 2007. Evaluation of blast-induced ground vibration predictors. *Soil Dynamics and Earthquake Engineering*, pp. 116-125.

[50] Monjezi, M., M. Ghafurikalajahi, and A. Bahrami, 2011. Prediction of blast-induced ground vibration using artificial neural networks. *Tunnelling and Underground Space Technology* 26.1, 46-50.

[51] Rodríguez, Rafael, Cristobal Lombardía, and Susana Torno, 2010. Prediction of the airwave due to blasting inside tunnels: approximation to a 'phonometric curve'. *Tunnelling and Underground Space Technology*, 25, 483-489.

[52] Khandelwal, Manoj, 2010. Evaluation and prediction of blast-induced ground vibration using support vector machine. International Journal of Rock Mechanics and Mining Sciences, ISSN 1365-1609, Volume 47, Issue 3, pp. 509 – 516.

[53] Nateghi, Reza, 2012. Evaluation of blast induced ground vibration for minimizing negative effects on surrounding structures. Soil Dynamics and Earthquake Engineering, 43, 133-138.

[54] Grundstrom, C., Kanchibotla, S., Jankovich, A., Thornton, D., & Pacific, D. D. N. A., 2001. Blast fragmentation for maximizing the sag mill throughput at Porgera Gold Mine. In proceedings of the annual conference on explosives and blasting technique, Vol. 1, pp. 383-400.

[55] U. Langefors, B. Kihlstrom, 1963. The modern technique of rock blasting. Wiley, New York.

[56] Cunningham C. V. B., 1983. The Kuz-Ram model for prediction of fragmentation from blasting, Lulea Fragmentation Conference, pp 439-454.

[57] National Association of Australian State Road Authorities, 1983. Explosives in Roadworks - A Users Guide, NAASRA, Sydney.

[58] KuznetsovV. M., 1973. The mean diameter of the fragments formed by blasting rock. Soviet Mining Science, 144-148.

[59] Segarra, P., et al., 2010. Prediction of near field overpressure from quarry blasting. *Applied Acoustics 71*(12), 1169-1176.

[60] P. Pal Roy, 2005. Rock blasting effects and operations. Balkema Publisher

[61] Gao, Fuqiang and Wang, Xiaoqiang, 2012. Using artificial neural network to predict blast-induced ground vibration. Applied Mechanics and Materials, ISSN 1660-9336, ISBN 9783037854228, Volume 170-173, pp. 1013 – 1016.

[62] Monjezi, M; Ahmadi, M; Sheikhan, M; Bahrami, A; Salimi, A.R, 2010. Predicting blast-induced ground vibration using various types of neural networks. Soil Dynamics and Earthquake Engineering, ISSN 0267-7261, Volume 30, Issue 11, pp. 1233 – 1236.

[63] Görgülü, K., Arpaz, E., Demirci, A., Koçaslan, A., Dilmaç, M. K., & Yüksek, A. G., 2013. Investigation of blast-induced ground vibrations in the Tülü boron open pit mine. *Bulletin of Engineering Geology and the Environment*, *72*(3-4), 555-564.

[64] Khandelwal, Manoj and Singh, T.N, 2006. Prediction of blast induced ground vibrations and frequency in opencast mine: A neural network approach. Journal of Sound and Vibration, ISSN 0022-460X, Volume 289, Issue 4, pp. 711 – 725.

[65] Mohamad, Edy Tonnizam; Noorani, Seyed Ahmad; Armaghani, Danial Jahed; Saad, Rosli, 2012. Simulation of blasting induced ground vibration by using artificial neural network. Electronic Journal of Geotechnical Engineering, EISSN 1089-3032, Volume 17, pp. 2571 – 2584.

[66] Kamali M. and Ataei M., 2010. Prediction of blast induced ground vibrations in Karoun III power plant and dam: a neural network. Journal of the South African institute of mining and metallurgy, ISSN 0038-223X, Volume 110, Issue 8, pp. 481 – 490.

[67] Lu, Yong, 2005. Underground blast induced ground shock and its modelling using artificial neural network. Computers and Geotechnics, ISSN 0266-352X, Volume 32, Issue 3, pp. 164 – 178.

[68] Faramarzi, F., Farsangi, M. A. E., & Mansouri, H., 2014. Simultaneous investigation of blast induced ground vibration and airblast effects on safety level of structures and human in surface blasting. *International Journal of Mining Science and Technology*, *24*(5), 663-669.

[69] Majdi, Abbas, and Mohammad Rezaei, 2013. Prediction of unconfined compressive strength of rock surrounding a roadway using artificial neural network. *Neural Computing and Applications* 23.2, 381-389.

[70] C.J. Konya, E.J. Walter, 1990.Surface blast design. Prentice Hall, Englewood Cliffs.

[71] Ranjith, P. G., and Manoj Khandelwal, 2012. Artificial neural network for prediction of air flow in a single rock joint." *Neural Computing and Applications* 21.6, 1413-1422.

[72] R. Rodríguez, J. Toraño, M. Menéndez, 2007. Prediction of the airblast wave effects near a tunnel advanced by drilling and blasting. Tunn Undergr Sp Technol, pp. 241–25.

[73] Leu, Sou-Sen, Chee-Nan Chen, and Shiu-Lin Chang, 2001. Data mining for tunnel support stability: neural network approach. *Automation in Construction* 10.4, 429-441.

[74] M.T. Mohamed. Performance of fuzzy logic and artificial neural network in prediction of ground and air vibrations, 2011. Int J Rock Mech Min Sci, 48, pp. 845–851.

[75] M. Khandelwal, T.N. Singh, 2005. Prediction of blast induced air overpressure in opencast mine. Noise and Vibration Control Worldwide, 36, pp. 7–16.

[76] E. Tonnizam Mohamad, M. Hajihassani, D. Jahed Armaghani, A. Marto, 2012. Simulation of blasting-induced air overpressure by means of artificial neural networks. Int Rev Modell Simulations, pp. 2501–2506.

[77] Meulenkamp, F., and M. Alvarez Grima, 1999. Application of neural networks for the prediction of the unconfined compressive strength (UCS) from Equotip hardness. *International Journal of rock mechanics and mining sciences*, 36.1, 29-39.

[78] Shahin, Mohamed A., Mark B. Jaksa, and Holger R. Maier, 2001. Artificial neural network applications in geotechnical engineering. *Australian Geomechanics*, 36.1, 49-62.

[79] Monjezi, M., Ahmadi, Z., Varjani, A. Y., and Khandelwal, M., 2013. Backbreak prediction in the Chadormalu iron mine using artificial neural network. *Neural Computing and Applications*, *23*(3-4), 1101-1107.

[80] Trivedi, R., T. N. Singh, and A. K. Raina, 2014. Prediction of blast-induced flyrock in Indian limestone mines using neural networks. *Journal of Rock Mechanics and Geotechnical Engineering*, 6.5, 447-454.

[81] Rosenblatt, Frank, 1958. The perceptron: a probabilistic model for information storage and organization in the brain. *Psychological review* 65.6, 386.

[82] Paley, N., and Kojovic, T., 2001. Adjusting blasting to increase SAG mill throughput at the Red Dog mine, Proc 27th ISEE Annual Conference, Orlando, January, pp. 65-80.

[83] Valery, W., Morrell, S., Kojovic, T., Kanchibotla, S.S., and Thornton, D.M., 2001. Modeling and Simulation Techniques Applied for Optimisation of Mine to Mill Operations and Case Studies", Proceedings - VI Southern Hemisphere Meeting on Mineral Technology, CETEM/MCT, Rio de Janeiro, Brazil, pp. 107-116.

[84] Werbos, P.J., 1975. Beyond Regression: New Tools for Prediction and Analysis in the Behavioral Sciences.

[85] Rumelhart, D.E; James McClelland, 1986. Parallel Distributed Processing: Explorations in the Microstructure of Cognition. Cambridge: MIT Press.

[86] Monjezi, M., Mehrdanesh, A., Malek, A., & Khandelwal, M., 2013. Evaluation of effect of blast design parameters on flyrock using artificial neural networks. *Neural Computing and Applications*, *23*(2), 349-356.

VITA

Raymond Ninnang Tiile was born in Upper West Region, Ghana. He holds a BS in Mining Engineering from the University of Mines and Technology, Tarkwa, Ghana. He is a young ambitious mining engineer with excellent technical training and working experience with a strong desire to take his career to greater heights.

After successfully attaining his bachelors, he gathered enormous training and experience working with a number of mining companies in Ghana namely; Strategic Mining Support services (SMiSS), AngloGold Ashanti mine, Maxam Explosive Limited and Perseus Mining Limited.

He subsequently gained admission to study MS in Mining Engineering at Missouri University of Science and Technology in Rolla, Missouri. During this period, he took a couple of graduate courses and served as a Graduate Research Assistant and Teaching Assistant. He was also an active member of different professional organizations including Society for Mining, Metallurgy and Exploration (SME) and Canadian Institute of Mining, Metallurgy and Petroleum (CIM).

Raymond graduated with MS Mining Engineering in July 2016.